Action Minimization and Sharp-Interface Limits for the Stochastic Allen-Cahn Equation

ROBERT V. KOHN
Courant Institute

FELIX OTTO
University of Bonn

MARIA G. REZNIKOFF
University of Bonn

AND

ERIC VANDEN-EIJNDEN
Courant Institute

Abstract

We study the action minimization problem that is formally associated to phase transformation in the stochastically perturbed Allen-Cahn equation. The sharp-interface limit is related to (but different from) the sharp-interface limits of the related energy functional and deterministic gradient flows. In the sharp-interface limit of the action minimization problem, we find distinct "most likely switching pathways," depending on the relative costs of nucleation and propagation of interfaces. This competition is captured by the limit of the action functional, which we derive formally and propose as the natural candidate for the Γ-limit. Guided by the reduced functional, we prove upper and lower bounds for the minimal action that agree on the level of scaling. © 2006 Wiley Periodicals, Inc.

Contents

Communications on Pure and Applied Mathematics, Vol. LIX, 0001–0046 (2006)

1 Introduction

At the mean field level, phase transformation can be studied within the framework of Ginzburg-Landau theory. It describes the state of the system in terms of a scalar order parameter u defined in a domain $\Omega \subset \mathbb{R}^d$ and a free energy

$$E^\varepsilon[u] = \int_\Omega \left(\frac{|\nabla u|^2}{2} + \varepsilon^{-2} V(u) \right) dx. \tag{1.1}$$

The gradient term penalizes spatial variation, and the potential V has a double-well shape with minima at the preferred states of the order parameter; the relative strength of the two terms is measured by the parameter ε. A canonical example of V is given by

$$V(u) = \frac{1}{4}(1-u^2)^2, \tag{1.2}$$

and for simplicity, we restrict our attention to this potential. Generalization to other choices of equal-well potentials for V is possible. (This changes the value of the constant c_0, which appears, for example, in Definitions 2.1 and 2.3 below.)

The L^2-gradient flow for (1.1) is the Allen-Cahn equation

$$\dot{u} = \Delta u - \varepsilon^{-2} V'(u). \tag{1.3}$$

(Throughout, $\dot{u}$ denotes the time derivative of u.) The only two stable fixed points of the dynamics (1.3) are the pure states $u_- \equiv -1$ and $u_+ \equiv +1$ (for periodic or Neumann boundary conditions). An energy barrier separates them, and initial conditions close to u_- never visit u_+.

As soon as thermal effects are taken into account, the picture changes. Even for small thermal noise, an initial state $u(\cdot, 0) = u_-$ will eventually undergo phase transformation (or "switching") driven over the energy barrier and into a small neighborhood of u_+. A natural way to include a noise term in (1.3) is via the stochastically perturbed Allen-Cahn equation:

$$\dot{u} = \Delta u - \varepsilon^{-2} V'(u) + \sqrt{2\gamma}\ \eta_\lambda. \tag{1.4}$$

Here γ is a parameter measuring the temperature of the system, and η_λ is a spatially regularized noise:

$$\eta_\lambda := \phi_\lambda * \eta,$$

where $*$ denotes convolution, $\phi_\lambda(x) = \lambda^{-d}\phi(x/\lambda)$ for ϕ an approximate identity, and η is a standard space-time white noise, i.e., a Gaussian process with mean zero and covariance $\mathbb{E}(\eta(x,t)\eta(x',t')) = \delta(x-x')\delta(t-t')$. The parameter λ measures the correlation length in the noise, and $\lambda = 0$ leads formally to an invariant measure that is the Gibbs distribution for the energy (1.1) with temperature γ.

The main objective of the paper is to study phase transformation in the sharp-interface limit, $\varepsilon \to 0$. The noise term in (1.4) introduces two additional parameters, γ and λ. We are interested in the limit in which all three parameters go to zero. The limit $\gamma \to 0$ is interesting because it is the small temperature regime in which the stochastic dynamics in (1.4) are not dominated by the noise term, but rather involve an interplay between the deterministic and stochastic parts. As mentioned above, the limit $\lambda \to 0$ is distinguished by being (formally) consistent with the Gibbs distribution. Finally, the sharp-interface limit, $\varepsilon \to 0$, leads to a reduced problem in which the switching pathway is characterized by the generation and propagation of interfaces (see below).

In this paper, we study a specific order of the limits; namely, we take $\gamma \to 0$ first, then $\lambda \to 0$, and finally $\varepsilon \to 0$. This limit is analytically accessible because it allows us to study the problem using large-deviation theory, and even though (1.4) is ill-posed for $\lambda = 0$ in dimension $d > 1$, it is possible to study $\lambda \to 0$ after first letting $\gamma \to 0$, as we explain in the following discussion. A more general analysis of the behavior of (1.4) in terms of $(\varepsilon, \gamma, \lambda)$ is an interesting but complicated topic. In Section 5, we comment briefly on the question of permuting the limits.

Large Deviations

The probability of a stochastically driven barrier-crossing event is estimated by the Wentzell-Freidlin theory of large deviations in terms of an *action functional*. If we define the set

$$\mathcal{A} := \{u(\,\cdot\,, 0) = u_-,\, u(\,\cdot\,, t) \in \mathrm{nbd}(u_+) \text{ for some } t \le T\},$$

then for $\gamma \ll 1$, the probability of switching under the dynamics (1.4) in time T is roughly estimated by

$$\mathrm{prob}(\mathcal{A}) \approx \exp\left(- \inf_{u \in \mathcal{A}} \frac{S^{\varepsilon,\lambda}[u]}{\gamma} \right), \tag{1.5}$$

where the action functional is

$$S^{\varepsilon,\lambda}[u] = \frac{1}{4} \int_0^T \int_\Omega \int_\Omega (\mathcal{F}u(x,t), K_\lambda^{-1}(x,y)\mathcal{F}u(y,t))\, dy\, dx\, dt, \tag{1.6}$$

for all u such that this quantity is defined, and infinity otherwise. Here, we have defined

$$\mathcal{F}u(x,t) := \dot{u}(x,t) - \Delta u(x,t) + \varepsilon^{-2} V'(u(x,t)),$$

and K_λ is the spatial covariance operator of η_λ, i.e.,

$$\mathbb{E}\,(\eta_\lambda(x,t)\eta_\lambda(y,t)) = K_\lambda(x-y)\delta(t-s).$$

Furthermore, the *minimizer* of the action functional over $\mathcal{A}$ is the *most likely switching pathway*, the deterministic trajectory that is approximated by the noisy path as it crosses the energy barrier (with probability 1, in the limit $\gamma \to 0$). For a complete discussion, see [7, 15, 38].

Taking the limit in (1.6) as the correlation length vanishes leads to

$$S^{\varepsilon}[u] = \frac{1}{4}\int_0^T \int_{\Omega} (\dot{u} - \Delta u + \varepsilon^{-2} V'(u))^2 \, dx \, dt. \tag{1.7}$$

In dimension $d = 1$, where the stochastic equation is well-defined even with a space-time white noise, Faris and Jona-Lasinio [13] prove that (1.7) is the action functional for (1.4) on the space of continuous functions. Although the stochastic PDE with $\lambda = 0$ is ill-posed in higher dimensions, the behavior of (1.7) controls the behavior of observables (such as the mean switching time between u_- and u_+) for $\lambda \ll 1$, at least in an appropriate regime of the $(\varepsilon, \gamma, \lambda)$ parameter space.

Motivated by these ideas, we study the action minimization problem

$$\inf_{\substack{u(\cdot,0)=u_- \\ u(\cdot,T)=u_+}} S^{\varepsilon}[u].$$

For simplicity, we focus on $\Omega = [0, L]^d$ and periodic boundary conditions. The cases of Neumann and homogeneous Dirichlet boundary conditions are conceptually the same, requiring only minor modification of the assertions; we comment occasionally on similarities and differences.

Sharp-Interface Limit: Deterministic

When $\varepsilon \ll 1$ in (1.1) or (1.3), the field u is forced to concentrate on ± 1 except possibly at sharp interfaces between the two phases. The so-called sharp-interface limit $\varepsilon \to 0$ corresponds to the limit of infinite scale separation between the interfacial length scale and the system size and has been studied previously both on the level of the energy functional, and the deterministic dynamics.

Any sequence u_ε with uniformly bounded renormalized energy,

$$\hat{E}^{\varepsilon}[u] := \varepsilon E^{\varepsilon}[u] = \int_{\Omega} \left(\frac{\varepsilon |\nabla u|^2}{2} + \varepsilon^{-1} V(u) \right) dx \tag{1.8}$$

converges as $\varepsilon \to 0$ (up to a subsequence) to a function that is a.e. ± 1, with an interface $\partial\{u = 1\}$ of finite perimeter. Moreover, Modica and Mortola [26, 27] proved the Γ-convergence of the renormalized energy to the perimeter functional,

$$\hat{E}^{\varepsilon}[\cdot] \xrightarrow{\Gamma} c_0 P[\cdot],$$

where here and throughout, the constant c_0 corresponding to the potential V defined in (1.2) is $c_0 := 2\sqrt{2}/3$. (In brief, Γ-convergence is a notion of convergence for variational problems which implies, in particular, that minimizers converge to minimizers of the limit problem, and which is stable under compact perturbations. See, for instance, [2].)

Given the Γ-convergence of the energy, one would like to know what becomes of the deterministic gradient flow in the sharp-interface limit. Is the limit of the gradient flow equal to the gradient flow for the limiting energy? It is known

[9, 12, 21, 35] that in dimension $d > 1$, (1.3) leads to limiting dynamics in which the interface $\partial\{u = 1\}$ evolves by mean curvature flow (MCF), i.e.,

$$v_n = -\kappa, \tag{1.9}$$

where v_n is the normal velocity of the interface and κ is the mean curvature. Because curvature flow is the gradient flow of the perimeter functional with respect to L^2 of the interface, we see that in this sense, the limiting dynamics are indeed the gradient flow of the limiting energy. (The change of metric — from L^2 in the bulk to L^2 on the interface — is related to the slowing down of the dynamics as $\varepsilon \to 0$.) In one space dimension, the situation is somewhat degenerate; here, the interfaces are points, and the slow motion of the interfaces has no effect on the leading-order term in the energy. Driven instead by the exponentially small correction terms in the energy, the interface motion is exponentially slow [4, 5, 17].

Sharp-Interface Limit: Action Functional

The central question in this paper is what happens to the renormalized action functional,

$$\hat{S}^\varepsilon[u] := \varepsilon S^\varepsilon[u] = \frac{1}{4}\int_0^T \int\limits_\Omega \left(\varepsilon^{1/2}\dot{u} + \varepsilon^{-1/2}(-\varepsilon\Delta u + \varepsilon^{-1}V'(u))\right)^2 dx\, dt \tag{1.10}$$

in the sharp-interface limit. We show that the (renormalized) minimum action

$$\hat{S}_{\text{switch}} := \inf_{\substack{u(\,\cdot\,,0)=u_-\\ u(\,\cdot\,,T)=u_+}} \hat{S}^\varepsilon[u] \tag{1.11}$$

remains bounded and nontrivial as $\varepsilon \to 0$ by developing ε-independent upper and lower bounds. Moreover, our upper-bound constructions suggest the following candidates for the Γ-limit of (1.10): In dimension $d > 1$, the candidate for the Γ-limit is

$$\frac{c_0}{4}\int_0^T \int\limits_{\Gamma(t)} (v_n + \kappa)^2\, d\sigma\, dt + S_{\text{nuc}}, \tag{1.12}$$

where S_{nuc} is the nucleation cost, $\Gamma(t)$ is the interface at time t, v_n is the normal velocity, and κ is curvature. (The nucleation cost is the jump in action that results from the energy jump if $(d-1)$–dimensional interfaces are generated.) We use our upper-bound constructions in Section 3.2 to prove that in $d = 2$, for instance, action-minimizing pathways *must* have higher-dimensional spatial structure (i.e., they cannot be merely one-dimensional).

The degeneracy in dimension $d = 1$ makes the situation slightly different. There is no notion of curvature, and the contribution of the energy vanishes in the limit. The candidate for the Γ-limit in $d = 1$ is

$$\frac{c_0}{4}\sum_{i=1}^N \int_0^T \dot{g}_i(t)^2\, dt + S_{\text{nuc}}, \tag{1.13}$$

where $g_i(t)$ is the position of the i^{th} interface at time t. Whereas in higher dimensions there is no nucleation cost for lower-dimensional interfaces (interfaces of dimension less than $d-1$), in dimension $d=1$ there is no possibility of avoiding a nucleation cost.

An elementary argument produces a lower bound that matches our upper bounds in terms of *scaling* (cf. Section 4.1). Proving sharp, ansatz-free lower bounds for (1.10) — which is necessary in order to justify the Γ-limit candidates suggested above — goes beyond the scope of this paper. We explain in Section 4.3, however, how the limiting behavior of the energy measures and equipartition between the bulk and gradient terms in the energy (1.8) are linked to proving a lower bound for the action functional. These ideas are used in [22] to prove rigorous results for the case $d=1$. (See Section 4.3 for a precise statement.) In some sense, it is not surprising that equipartition of energy plays a role in the action problem, since it is important in proving convergence of the Allen-Cahn dynamics to Brakke's notion of curvature flow [21].

Is the sharp-interface limit of the action functional the action functional of sharp-interface gradient flow? Formally, we give a positive answer by identifying the limiting action, (1.12). Indeed, given a gradient flow, one can view the Γ-convergence of the associated energy functional and the (nondegenerate) Γ-convergence of the decoupled action functional (1.18) as sufficient conditions for the convergence of the dynamics to the gradient flow for the limiting energy, much in the spirit of Sandier and Serfaty [36].

On the deeper level of the stochastic problem, one would like to know whether this limiting action is in fact the action functional for a well-defined stochastic process and, moreover, whether this process is the sharp-interface limit of the process defined by (1.4). See Section 5 for a few additional comments.

Initial Observations and Heuristics

We conclude the introduction by explaining some basic properties of the action functional and the heuristic picture for $d=1$. In particular, we explain the connection between the energy and action functionals, and how a competition between the costs of forming and transporting interfaces emerges in the sharp-interface limit.

The most fundamental relationship between the action and energy functionals is revealed by the fact that for any $t \in (0,T]$

$$\begin{aligned}\hat{S}^\varepsilon[u] &\geq \frac{1}{4}\int_0^t \int_\Omega \left(\varepsilon^{1/2}\dot{u} + \varepsilon^{-1/2} D_u \hat{E}^\varepsilon(u)\right)^2 dx\, dt' \\ &= \frac{1}{4}\int_0^t \int_\Omega \left(\left(\varepsilon^{1/2}\dot{u} - \varepsilon^{-1/2} D_u \hat{E}^\varepsilon(u)\right)^2 + 4\dot{u}\, D_u \hat{E}^\varepsilon(u)\right) dx\, dt' \\ &\geq \hat{E}^\varepsilon[u(\cdot,t)] - \hat{E}^\varepsilon[u(\cdot,0)]. \end{aligned} \tag{1.14}$$

(We have used $D_u\hat{E}^\varepsilon := -\varepsilon\Delta u + \varepsilon^{-1}V'(u)$ as shorthand for the functional derivative of the energy in L^2, and in the third line we have used the boundary conditions to integrate by parts.) An immediate consequence is that the minimal action is bounded below by the energy barrier between u_- and u_s, the minimum-energy saddle point (which we will also call the minimal saddle):

$$\hat{S}_{\text{switch}} \geq \hat{E}^\varepsilon[u_s] - \hat{E}^\varepsilon[u_-] =: \Delta\hat{E}^\varepsilon. \tag{1.15}$$

(For periodic or Neumann boundary conditions, the barrier is exactly equal to the energy of u_s; for zero Dirichlet boundary conditions, there is a correction due to the nonzero energy of u_-.) Looked at from a slightly different point of view, (1.14) shows that functions with bounded action are bounded in energy at every time $t \leq T$. Thus, while action minimizers are not energy minimizers, their energy is uniformly bounded in time.

The calculation in (1.14) also characterizes the long-time action minimizing trajectory in terms of the deterministic Allen-Cahn dynamics. An action that is strictly *equal* to the energy barrier can only be achieved by a path that flows through the minimal saddle and satisfies

$$\dot{u} = \begin{cases} +\varepsilon^{-1}D_u\hat{E}^\varepsilon(u), & t \leq T^*, \\ -\varepsilon^{-1}D_u\hat{E}^\varepsilon(u), & T^* < t \leq T, \end{cases} \tag{1.16}$$

with

$$u(\,\cdot\,,0) \equiv -1, \quad u(\,\cdot\,,T^*) = u_s, \quad u(\,\cdot\,,T) \equiv +1. \tag{1.17}$$

Indeed, (1.16) and (1.17) give

$$\begin{aligned}
&\frac{1}{4}\int_0^{T^*}\int_\Omega \left(\varepsilon^{1/2}\dot{u} + \varepsilon^{-1/2}D_u\hat{E}^\varepsilon(u)\right)^2 dx\,dt' \\
&= \frac{1}{4}\int_0^{T^*}\int_\Omega \left(\left(\varepsilon^{1/2}\dot{u} - \varepsilon^{-1/2}D_u\hat{E}^\varepsilon(u)\right)^2 + 4\dot{u}\,D_u\hat{E}^\varepsilon(u)\right)dx\,dt' \\
&= \hat{E}^\varepsilon[u(\,\cdot\,,T^*)] - \hat{E}^\varepsilon[u(\,\cdot\,,0)] \\
&= \hat{E}^\varepsilon[u_s]
\end{aligned}$$

and

$$\frac{1}{4}\int_{T^*}^{T}\int_\Omega \left(\varepsilon^{1/2}\dot{u} + \varepsilon^{-1/2}D_u\hat{E}^\varepsilon(u)\right)^2 dx\,dt' = 0.$$

(We remark that the first part of (1.16) is well-posed only as a boundary value problem connecting u_- and u_s.) Such an "ideal" pathway requires infinite time, but for switching times that are large compared to the deterministic timescale, an approximation of the pathway (modified near the critical points) achieves a nearly optimal action; see, for instance, the proof of Proposition 3.1.

When the switching time T is short compared to the deterministic timescale, on the other hand, the action minimization problem is more complicated. The sharp-interface limit is a regime in which the full action minimization problem reduces to a competition between two costs: the cost to form interfaces and the cost to move them. We call the former the nucleation cost and the latter the propagation cost. (We use the term *nucleation* in a loose sense here; see Remark 1.1 below.) The action-minimizing trajectory strikes an optimal balance between these costs, depending on the relative size of the switching time T and the system size L. The phenomenon of competing nucleation and propagation costs was studied in [10] and also (for $d = 1$) in [14]; the same phenomenon is also investigated for a different but related one-dimensional model in [8].

To capture the main idea of the competition between nucleation and propagation costs in the action, consider the case $d = 1$. Each point nucleation incurs a cost. On the other hand, moving the interfaces across the system within time T also incurs a cost, and the more interfaces there are, the less distance that each must travel. (See Figure 3.1.) The back-of-the-envelope calculation that compares these two costs is the following: Assume a fixed cost per nucleation and a periodic structure, so that there are L/ℓ nucleations, spaced ℓ apart. The nucleation cost is $\sim L/\ell$. Estimating the propagation cost by the transportation term in the action yields a cost $\sim L\ell/T$. Balancing these costs implies $\ell = \sqrt{T}$, and a minimal action that scales like $L/\sqrt{T}$.

Finally, the boundary conditions and the initial and final conditions also imply that the action decouples as

$$\begin{aligned}&\frac{1}{4}\int_0^T \int_{\Omega} \left(\varepsilon^{1/2}\dot{u} + \varepsilon^{-1/2} D_u \hat{E}^{\varepsilon}(u)\right)^2 dx\, dt \\ &\quad = \frac{1}{4}\int_0^T \int_{\Omega} \left(\varepsilon \dot{u}^2 + \varepsilon^{-1}(D_u \hat{E}^{\varepsilon}(u))^2\right) dx\, dt.\end{aligned}$$

The penalization of the second term suggests using hyperbolic tangent profiles or, more precisely, using constructions in which $u(x,t)$ is defined in terms of the hyperbolic tangent of the distance from x to the interface $\Gamma(t)$; cf. Section 2.

Two Other Scaling Regimes

Given the action functional

$$S^{L,T}[u] := \int_0^T \int_{\Omega_L} \left(\dot{u} - \Delta u + V'(u)\right)^2 dx\, dt, \tag{1.18}$$

one passes to the sharp-interface regime by considering $L \to \infty$, $T \to \infty$, with the diffusive scaling $L \sim \sqrt{T} =: \varepsilon^{-1}$. This is the most interesting scaling, because of the competition between nucleation cost and propagation cost. More generally, however, the minimization problem

$$S_{\text{switch}} := \inf_{\substack{u(\,\cdot\,,0)=u_- \\ u(\,\cdot\,,T)=u_+}} S^{L,T}[u]$$

is an implicit function of the two parameters L and T, and other limits may of course also be considered. We point out two additional scaling regimes of the action, the short-time limit ($T \to 0$ with L fixed) and the energy barrier regime ($L, T \to \infty$ with $L \ll \sqrt{T}$). These regimes are easy to understand; see Appendix A.

In the energy barrier regime, the action depends on the minimum-energy saddle point, which in turn depends on the system size. We study this dependence in Appendix B. In particular, we look at the crossover in the energy-minimizing saddle point from $u \equiv 0$ to a spatially nonuniform saddle, and at the limiting energy of this minimal saddle, as the domain becomes large (or equivalently as ε vanishes).

Organization

In Section 2, we present the reduced action functional and a heuristic derivation. We will prove the *scaling* of the action in the sharp-interface regime by developing matching upper and lower bounds. In Section 3, we introduce the upper bound constructions. For $d > 1$, we introduce one-dimensional, mean-curvature-flow, and accelerated mean-curvature-flow constructions. In Section 4, we turn to the question of lower bounds. We prove a lower bound for the scaling and investigate what would be necessary in order to improve the result to a sharp bound. In Section 5 we conclude with some additional connections and open problems. In Appendix A we consider two (simple) limits other than the sharp-interface limit, namely, the short-time limit and the energy-barrier regime. Finally, in Appendix B, we study the dependence of the energy on the system size.

Remark 1.1. We use the term *nucleation* to mean the nucleation of a new phase. Classically, the term *nucleation event* is often used to mean passing through a saddle point. In the case where V is an asymmetric double-well potential, for instance, the minimum-energy saddle point is a droplet that is localized, and nucleation refers to passing through this well-defined point in phase space. In the setting of the symmetric double well, there is no localized droplet, or, in other words, the minimum-energy saddle point does not converge as the system size goes to infinity. For us, nucleation means the generation of an interface connecting $u \approx -1$ with $u \approx +1$.

2 The Reduced Action Functional

In this section, we present the candidate for the Γ-limit of the renormalized action functional (1.10). One can view our argument either as a formal derivation

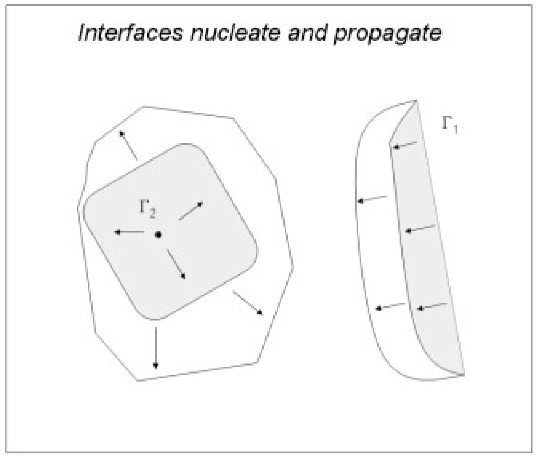

FIGURE 2.1. Interfaces forming and propagating in a two-dimensional system. The reduced action functional counts the perimeter of nucleated structures and the propagation cost of moving against curvature.

or as a building block for the upper-bound half of a Γ-limit argument. (We use the structure of the reduced action functional to develop upper-bound constructions in Section 3.) A matching lower bound requires an analysis of the limiting energy measures; see Section 4 and also [22] for $d = 1$.

We begin with a definition.

DEFINITION 2.1 The *reduced action functional* for the family of interfaces $\Gamma(t)$, $t \in [0, T]$, is

$$S^R[\Gamma(\cdot)] := S^R_{\text{prop}}[\Gamma(\cdot)] + S^R_{\text{nuc}}[\Gamma(\cdot)], \tag{2.1}$$

where

$$S^R_{\text{prop}}[\Gamma(\cdot)] := \frac{c_0}{4}\int_0^T \int_{\Gamma(t)} (v_n + \kappa)^2 \, d\sigma \, dt, \quad S^R_{\text{nuc}}[\Gamma(\cdot)] := 2c_0 \sum_i \mathcal{H}^{d-1}(\Gamma_i).$$

Here, v_n and κ are the normal velocity and curvature of the interface. In $d = 1$ we take the curvature of a point to be zero by definition. $\mathcal{H}^{d-1}$ represents the $(d-1)$–dimensional Hausdorff measure, and Γ_i is the i^{th} connected component of the interface at the time of creation of that component. (See Figure 2.1.)

PROPOSITION 2.2 *For $\varepsilon \to 0$, let $u_\varepsilon(x, t)$ be a periodic, action-minimizing sequence whose zero level sets converge to the smooth family of interfaces $\Gamma(t)$. Suppose that*

$$u_\varepsilon(x, 0) \equiv -1, \quad u_\varepsilon(x, T) \equiv +1,$$

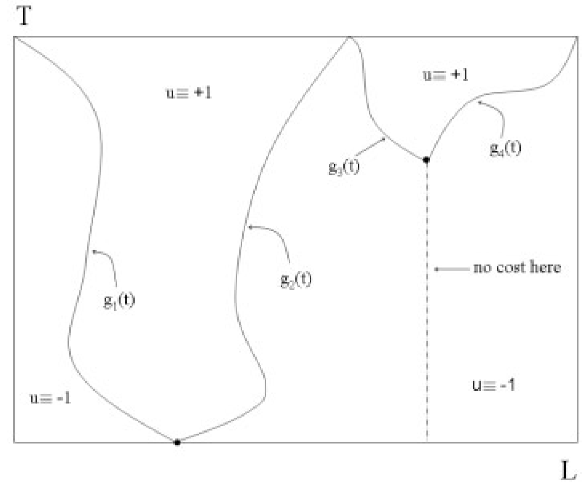

FIGURE 2.2. A space-time view of the sharp-interface limit of a switching path in one dimension. There are two nucleation events, and the interfaces propagate in order to achieve switching by the switching time $t = T$.

and that away from nucleation times, u_ε is of the form

$$u_\varepsilon(x,t) = v(\varepsilon^{-1} d(x, \Gamma(t))), \tag{2.2}$$

(*where $d(\cdot)$ is the signed distance function*). *Then formally*

$$\lim_{\varepsilon \to 0} \hat{S}_\varepsilon[u_\varepsilon] = S^R[\Gamma(\cdot)].$$

It is worth distinguishing the higher-dimensional case from the one-dimensional case. In $d > 1$, low-dimensional nucleations are possible that incur no nucleation cost ($S^R_{\text{nuc}}[\Gamma(\cdot)] = 0$). In contrast, for $d = 1$, nucleation cost is unavoidable. We emphasize the structure for $d = 1$ in a separate corollary.

DEFINITION 2.3 The *reduced action functional* in one dimension is given by

$$S^R[g(\cdot)] := \sum_{i=1}^{2N} \frac{c_0}{4} \int_0^T \dot{g}_i(t)^2 \, dt + 2Nc_0. \tag{2.3}$$

Here, the interface is a finite collection of time-dependent points $g(t) = \{g_i(t)\}_{i=1}^{2N}$, where the $g_i(t)$ give the location of the i^{th} interface at time t. (See Figure 2.2.)

COROLLARY 2.4 (One Dimension) *Suppose that $u_\varepsilon(x,t)$ is a periodic, action-minimizing sequence that satisfies the initial and final conditions and that away from nucleation times,*

$$u_\varepsilon(x,t) = v(\varepsilon^{-1} d(x, g(t))).$$

Then formally,

$$\lim_{\varepsilon\to 0} \hat{S}_\varepsilon[u_\varepsilon] = S^R[g(\cdot)].$$

PROOF OF PROPOSITION 2.2: We give a formal derivation of the reduced action functional. (An even simpler argument is possible for $d = 1$ by using the ansatz from the corollary.) For the nucleation cost S^R_{nuc}, we use a local estimate. Suppose that at time t_0 there is the nucleation of a $(d-1)$–dimensional curve Γ_i of $u \approx +1$ in a region of $u \approx -1$. The action cost for such an event is bounded below by the energy of the nucleated state, which converges to $2c_0\mathcal{H}^{d-1}(\Gamma_i)$ in the sharp-interface limit. Furthermore, this minimal cost can be achieved by reversing time along the heteroclinic orbit (as in the proof of Proposition 3.1, for instance).

To derive S^R_{prop}, substitute (2.2) into the normalized functional $\hat{S}^\varepsilon[u]$. We deduce $v(z) = \tanh(z/\sqrt{2})$ so that the highest-order terms vanish. (We assume $\Gamma(t)$ is a union of closed curves and take the convention that distance is positive if and only if the point is interior to one of the curves. This is consistent with functions that nucleate regions of $+1$.) We use the properties of the distance function

$$|\nabla d| = 1, \quad \Delta d\,|_{\Gamma(t)} = -\kappa, \quad \frac{d}{dt}\,d(x,\Gamma(t)) = v_n,$$

to derive

$$\begin{aligned}
\hat{S}^\varepsilon[u] &\approx \frac{\varepsilon^{-1}}{8}\iint \operatorname{sech}^4\left(\frac{d(x,\Gamma(t))}{\varepsilon\sqrt{2}}\right)(v_n+\kappa)^2\,dx\,dt \\
&= \frac{\varepsilon^{-1}}{8}\int_0^T\int_{s=-\infty}^{\infty}\int_{d=s} \operatorname{sech}^4\left(\frac{s}{\varepsilon\sqrt{2}}\right)(v_n+\kappa)^2\mathcal{H}^0(d^{-1}(s)\cap\Omega)d\sigma\,ds\,dt \\
&= \frac{\varepsilon^{-1}}{8}\int_0^T\int_{s=-\infty}^{\infty} \operatorname{sech}^4\left(\frac{s}{\varepsilon\sqrt{2}}\right)\int_{d=s}(v_n+\kappa)^2\mathcal{H}^0(d^{-1}(s)\cap\Omega)d\sigma\,ds\,dt,
\end{aligned}$$

where σ is the variable along the level curves of d, and the second-to-last equality follows by the co-area formula and the fact that $|\nabla d| = 1$. The multiplicity function $\mathcal{H}^0$ restricts the integration to the spatial domain. Now, because the hyperbolic secant is sharply peaked, Laplace's method indicates that

$$\begin{aligned}
\hat{S}^\varepsilon[u] &\approx \frac{\varepsilon^{-1}}{8}\int_0^T\int_{\Gamma(t)}(v_n+\kappa)^2\,d\sigma\int_{s=-\infty}^{\infty}\operatorname{sech}^4\left(\frac{s}{\varepsilon\sqrt{2}}\right)\mathcal{H}^0(d^{-1}(s)\cap\Omega)ds\,dt \\
&\underset{\varepsilon\to 0}{\to} \frac{c_0}{4}\int_0^T\int_{\Gamma(t)}(v_n+\kappa)^2\,d\sigma\,dt.
\end{aligned}$$

□

The reduced functionals help us to develop upper-bound constructions in Section 3.

3 Upper Bounds: Constructions

In this section, we develop upper bounds for the action in $d = 1$ and $d > 1$ by building constructions or test functions. Recall that the action is an infimum over all admissible functions. Thus, it is less than or equal to the cost for any specific construction. Moreover, a "good" construction gives a "good" bound. A perfect upper bound is one that is precisely matched by an ansatz-free lower bound. We will turn to the question of lower bounds in Section 4.

3.1 Dimension $d = 1$

The one-dimensional reduced action functional (2.3) reflects a cost for each nucleation point and a cost for propagation. The lowest cost is achieved by choosing equally spaced nucleation events and walls that propagate linearly in time. The constraint of switching means that the walls must cover the entire system by $t = T$ so that $g_1(T) = 0$ and $g_{2N}(T) = L$. (See Figure 3.1 for an illustration.) The optimal number of walls minimizes

$$c_0\left(2N + \frac{L^2}{8NT}\right). \tag{3.1}$$

We use these ideas in the one-dimensional upper bound construction.

PROPOSITION 3.1 (Upper Bound, $d = 1$) *For periodic boundary conditions and* $d = 1$*,*

$$\limsup_{\varepsilon\to 0} \hat{S}_{\text{switch}} \le \min_{N\in\mathbb{N}} \left(2N + \frac{L^2}{8NT}\right)c_0.$$

The corresponding assertion for Neumann boundary conditions follows easily:

COROLLARY 3.2 *For Neumann boundary conditions and* $d = 1$*,*

$$\limsup_{\varepsilon\to 0} \hat{S}_{\text{switch}} \le \min_{N\in\mathbb{N}} \left(N + \frac{L^2}{4NT}\right)c_0.$$

PROOF: We find it convenient to rescale space and time

$$\hat{x} := \frac{x}{\varepsilon}, \quad \hat{t} := \frac{t}{\varepsilon^2},$$

and work with the ε-independent functional

$$S[u] := \int_0^{\hat{T}} \int_0^{\hat{L}} (\dot{u} - u_{\hat{x}\hat{x}} + V'(u))^2 \, d\hat{x}\, d\hat{t}$$

in the limit $\hat{T} \to \infty$, $\hat{L} \to \infty$. Note that the ratio $\hat{L}/\sqrt{\hat{T}} = L/\sqrt{T}$ is preserved. For ease of notation, we drop the hats.

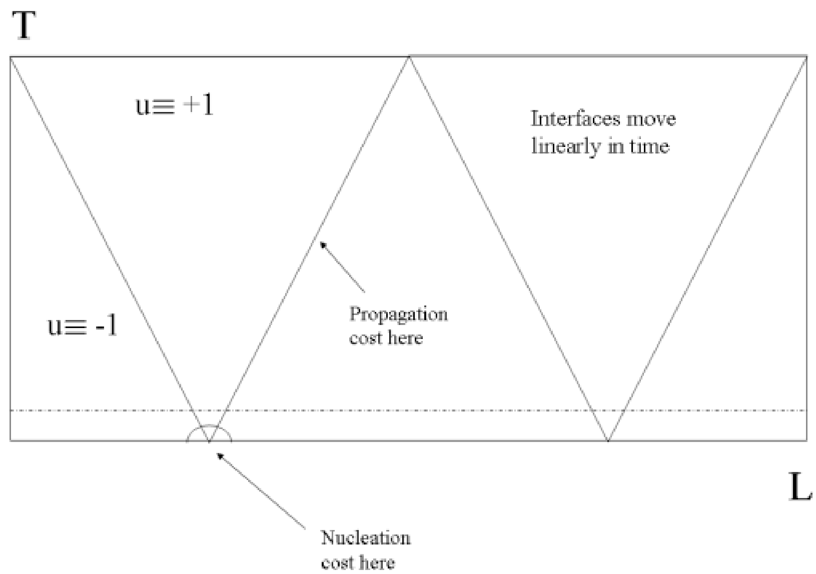

FIGURE 3.1. Action minimizer for $L = 8\sqrt{T}$.

Let $S_{[0,T]}$ denote the action on $[0, T]$. We need to show that for all $\delta > 0$, there exists a time T^* such that for all $T \geq T^*$,

$$\inf_u S_{[0,T]}[u] \leq \min_{N \in \mathbb{N}} \left(2N + \frac{L^2}{8NT} \right) c_0 + \delta.$$

We do this via explicit construction, demonstrating

$$\begin{aligned} &\forall \delta > 0,\ \exists T^* \text{ such that} \\ &\forall T \geq T^*,\ \exists u^{\delta,T} \text{ such that} \\ &S_{[0,T]}[u^{\delta,T}] \leq \min_{N \in \mathbb{N}} \left(2N + \frac{L^2}{8NT} \right) c_0 + \delta. \end{aligned}$$

Our test function will consist of N periodic cells of length $2\tilde{L} = L/N$. At the center of each cell is a nucleation point. Consider the action on a single cell, where we center the construction at $x = 0$ and take the system to be $[-\tilde{L}, \tilde{L}]$.

The construction proceeds in five stages. We first describe the stages and then explain how the parameters are chosen. We make use of the "nucleation state"

$$u_n(x) := \begin{cases} \tanh\left(\dfrac{L_1 + x}{\sqrt{2}}\right), & x \le 0, \\ \tanh\left(\dfrac{L_1 - x}{\sqrt{2}}\right), & x > 0, \end{cases}$$

where $L_1 < \tilde{L}/2$ is a free parameter of the construction, discussed below. Note that u_n has a jump in the derivative at $x = 0$. For a first pass, we ignore this problem and present the main idea of the estimates. We then demonstrate that the discontinuity can be smoothed without loss. The same is true for the discontinuity that comes from gluing two cells together.

Overview of the Five Stages

Stage 1. In time T_0, linearly interpolate from $u \equiv -1$ to u_0, a point on the orbit connecting (in infinite time) u_n with $u \equiv -1$ under the dynamics $\dot{u} = u_{xx} - V'(u)$. (As long as $L_1 < \tilde{L}/2$, u_n is in the basin of attraction of $u \equiv -1$, so this orbit exists. Actually, we will choose $L_1 < \tilde{L}/4$ for (3.2) below.)

Stage 2. In time T_1, follow the orbit from u_0 to u_n with time-reversed dynamics.

Stage 3. In time $T_2 := T - 2T_0 - 2T_1$, propagate the hyperbolic tangent profiles, using $u(x,t) := v(x, t - T_1 - T_0)$, with

$$v(x,t) := \begin{cases} \tanh\left(\dfrac{L_1 + x + ct}{\sqrt{2}}\right), & x \le 0, \\ \tanh\left(\dfrac{L_1 - x + ct}{\sqrt{2}}\right), & x > 0, \end{cases}$$

where $c := (\tilde{L} - 2L_1)/T_2$ so that the zeros of the tangents reach $\pm(\tilde{L} - L_1)$ by the end of propagation.

Stage 4. In time T_1, follow the orbit from this state to a point arbitrarily near $u \equiv +1$. (This is symmetric to stage 2 except that we follow the orbit in forward time.)

Stage 5. In time T_0, linearly interpolate to $u \equiv +1$.

Choice of Parameters and Action Cost

As in (1.14), the action cost in the second stage is $(E(u_n) - E(u_0)) \le E(u_n)$. The energy of u_n on each half-line converges monotonically as $L_1 \to \infty$, which comes from calculating

$$\int_{-b}^{b} \frac{1}{2}\left(\partial_x \tanh\left(\frac{x}{\sqrt{2}}\right)\right)^2 + \frac{1}{4}\left(1 - \tanh^2\left(\frac{x}{\sqrt{2}}\right)\right)^2 dx \underset{b\to\infty}{\uparrow} \frac{2\sqrt{2}}{3},$$

which we do by using u-substitution with $u(x) := \tanh(x/\sqrt{2})$ and applying the identity $u'(x) = (1 - u^2)/\sqrt{2}$. Therefore, the action of this stage is bounded by

$2 \times 2\sqrt{2}/3$. Fix L_1. (When we patch the function near $x = 0$ we will choose $L_1 \gg 1$ to control the error.)

Now choose u_0 on the orbit between -1 and u_n (corresponding to the L_1 chosen above) such that u_0 is not identically -1 and the action cost of the linear interpolation in stage 1 is less than $\delta/(4N)$. We use the lemma of Faris and Jona-Lasinio [13]:

LEMMA 3.3 (Faris and Jona-Lasinio) *For the linear interpolant*

$$u(t) := u(a)\left(1 - \frac{t}{\tau}\right) + u(b)\frac{t}{\tau}$$

with $u(a)$ *and* $u(b)$ *uniformly bounded and*

$$\|D_u E[u(a)]\|_{L^2} < \infty, \quad \|D_u E[u(b)]\|_{L^2} < \infty,$$

there exists a constant $c < \infty$ *and a* $T_0 \in (0, \infty)$ *such that the corresponding* u *satisfies*

$$S_{[0,T_0]}[u] \leq 2c\|u(a) - u(b)\|_{L^2}.$$

The proof is by separating the action as in (1.18). The time derivative is controlled by

$$\frac{\|u(a) - u(b)\|_{L^2}^2}{\tau},$$

and $\|D_u E[u(t)]\|_{L^2}$ is estimated in terms of the end states plus a bounded function, so that the second term in (1.18) is bounded by

$$C\tau.$$

Optimizing on τ completes the proof. By the lemma, it is possible to interpolate with a low cost, and there is a corresponding (small and finite) time T_0, which is optimal.

Next, find the time T_1 needed to connect states u_n and u_0. Note that T_1 is finite but large. According to a theorem of Carr and Pego [5], $T_1 \approx e^{2\sqrt{2}L_1}$.

Finally, consider the action for the propagation phase, stage 3. Here, the propagation action on each cell is bounded by

$$\begin{aligned}
\frac{\sqrt{2}}{3}c^2 T_2 &= \frac{\sqrt{2}}{3}\left(\frac{\tilde{L} - 2L_1}{T_2}\right)^2 T_2 \\
&= \frac{\sqrt{2}}{3}\frac{(\tilde{L} - 2L_1)^2}{T_2} \\
&\leq \frac{\sqrt{2}}{3}\frac{\tilde{L}^2}{T - 2T_0 - 2T_1} \\
&= \frac{\sqrt{2}}{12}\frac{L^2/N^2}{T - 2T_0 - 2T_1}
\end{aligned}$$

for $\tilde{L} \geq 2L_1$. Thus, multiplying by N, the total propagation action for T^* sufficiently large satisfies the bound

$$\begin{aligned} S_{[T_0+T_1, T-(T_0+T_1)]}[u] &\leq \frac{\sqrt{2}}{12}\frac{L^2}{NT}\left(1 - \frac{2(T_0+T_1)}{T}\right)^{-1} \\ &\leq \frac{\sqrt{2}}{12}\frac{L^2}{NT} + \frac{\delta}{4}. \end{aligned}$$

Now for any $T \geq T^*$, let u be constructed as outlined, with the given choices for u_0, T_0, L_1, and T_1. Then the total action is bounded as

$$\begin{aligned} S_{[0,T]}[u] &\leq \frac{\delta}{4} + \frac{4\sqrt{2}}{3}N + \left(\frac{\sqrt{2}}{12}\frac{L^2}{NT} + \frac{\delta}{4}\right) + \frac{\delta}{4} \\ &\leq \frac{4\sqrt{2}}{3}N + \frac{\sqrt{2}}{12}\frac{L^2}{NT} + \delta \\ &= \left(2N + \frac{L^2}{8NT}\right)c_0 + \delta. \end{aligned}$$

Minimizing over N completes the argument.

Smoothing the Discontinuity

We now return to the discontinuity in the derivative of the test function at $x = 0$, which we have ignored up to now. We use the fact that the discontinuity vanishes as $L_1 \to \infty$. Consider a smooth function $\phi : \mathbb{R} \to \mathbb{R}$ such that $\phi(x) \equiv 1$ for $x \leq -1$, $\phi(x) \equiv 0$ for $x \geq 1$, and ϕ and its derivatives are bounded by 1. Define the smooth nucleation state

$$\tanh\left(\frac{x+L_1}{\sqrt{2}}\right)\phi\left(\frac{x}{a}\right) + \tanh\left(\frac{-x+L_1}{\sqrt{2}}\right)\left(1 - \phi\left(\frac{x}{a}\right)\right)$$

for a small constant a. We will show that the estimate for the cost of the action in stage 2 remains valid. Let $\mathcal{E}u := (\partial_x u)^2/2 + (1-u^2)^2/4$. Then

$$\begin{aligned} E(u_n) = &\int_{-\tilde{L}}^{-a} \mathcal{E}\left(\tanh\left(\frac{x+L_1}{\sqrt{2}}\right)\right)dx \\ &+ \int_a^{\tilde{L}} \mathcal{E}\left(\tanh\left(\frac{-x+L_1}{\sqrt{2}}\right)\right)dx + \int_{-a}^{a} \mathcal{E}(u_n)dx. \end{aligned}$$

The first two integrals are bounded by $2\sqrt{2}/3$ as before, and the last integral vanishes as $a \to 0$ by virtue of the fact that

$$\left|\left(\tanh\frac{x+L_1}{\sqrt{2}}\right) - \tanh\left(\frac{-x+L_1}{\sqrt{2}}\right)\right| \leq C|x|$$

for $x \in [-a, a]$.

In stage 3 we let

$$v(x,t) := \tanh\left(\frac{x+L_1+ct}{\sqrt{2}}\right)\phi\left(\frac{x}{a}\right) + \tanh\left(\frac{-x+L_1+ct}{\sqrt{2}}\right)\left(1-\phi\left(\frac{x}{a}\right)\right).$$

We need to check the behavior of the action for $x \in [-a,a]$. The bound on the propagation term on this interval holds as before. To deal with the other term, we use $(u_{xx}+u-u^3)^2 \le 2u_{xx}^2 + 2(u-u^3)^2$. For the $u-u^3$ term, notice that u is a convex combination of the values of the two hyperbolic tangents, and on $[-a,a]$,

$$1 \ge u \ge \tanh\left(\frac{L_1-1+ct}{\sqrt{2}}\right) =: 1-\delta.$$

To complete the bound, we will also need to bound the wall speed from below. To this end, recall the definition

$$c := \frac{\tilde{L}-2L_1}{T_2}$$

and the relationships $L_1 \le \tilde{L}/4$, $\hat{L} = L/2N$, and $N \sim L/\sqrt{T}$. We estimate

$$c \ge \frac{\tilde{L}}{2T_2} \ge \frac{\tilde{L}}{2T} = \frac{L}{4NT} \gtrsim \frac{1}{\sqrt{T}}. \tag{3.2}$$

With these estimates in hand,

$$\begin{aligned} 2\int_{T_0+T_1}^{T-T_0-T_1}\int_{-a}^{a}(u-u^3)^2\,dx &\le 2\int_0^T\int_{-a}^{a}(4\delta)^2\,dx\,dt \quad \text{(for } \delta \text{ sufficiently small)}\\ &\lesssim a\int_0^T e^{-2\sqrt{2}(L_1-1+ct)}dt\\ &\lesssim \frac{ae^{-2\sqrt{2}L_1}}{c}\\ &\lesssim ae^{-2\sqrt{2}L_1}\sqrt{T}. \end{aligned}$$

We control this term by choosing $\sqrt{T} \ll e^{2\sqrt{2}L_1}$. Note that since increasing L_1 forces an exponential increase in T_1 (as $e^{2\sqrt{2}L_1}$), it is critical that we can satisfy $T^{1/2} \ll T_1 \ll T$. Because this is no problem for $T \to \infty$, given any δ, choosing T^* large enough suffices to secure the estimates.

Finally, consider the u_{xx}^2 term. On $[-a,a]$, u_{xx} is a rather long expression that we refrain from writing in full, but the worst term is the one in which both derivatives fall on ϕ, which we bound in the following way:

$$\begin{aligned} &\int_0^{T_2}\int_{-a}^{a}\left|a^{-2}\phi''\left(\frac{x}{a}\right)\left(\tanh\left(\frac{x+L_1+ct}{\sqrt{2}}\right) - \tanh\left(\frac{-x+L_1+ct}{\sqrt{2}}\right)\right)\right|^2 dx\,dt\\ &\quad\le a^{-4}\int_0^{T_2}\int_{-a}^{a}\left|\tanh\left(\frac{x+L_1+ct}{\sqrt{2}}\right) + \tanh\left(\frac{x-L_1-ct}{\sqrt{2}}\right)\right|^2 dx\,dt \end{aligned}$$

$$
\begin{aligned}
&\le 2a^{-4}\int_0^{T_2} \operatorname{sech}^4\left(\frac{L_1-1+ct}{\sqrt{2}}\right)\int_{-a}^{a} x^2\,dx\,dt \\
&= \frac{4a^{-1}}{3}\int_0^{T_2} \operatorname{sech}^4\left(\frac{L_1-1+ct}{\sqrt{2}}\right)dt \\
&\le \frac{64a^{-1}}{3}\int_0^{T_2} e^{-2\sqrt{2}(L_1-1+ct)}\,dt \\
&= \frac{64a^{-1}e^{-2\sqrt{2}(L_1-1)}}{6\sqrt{2}c}(1-e^{-2\sqrt{2}\,c\,T_2}) \\
&\lesssim \frac{a^{-1}}{c}\,e^{-2\sqrt{2}L_1} \\
&\lesssim \frac{T^{1/2}}{a}\,e^{-2\sqrt{2}L_1}.
\end{aligned}
$$

As before, we control this term by choosing L_1 sufficiently large. □

3.2 Higher Space Dimensions

The Γ-limit candidates (2.1) and (2.3) help us to develop upper bound constructions for $d > 1$. Using the reduced functional to conjecture how the interfaces of reduced action minimizers should behave, we build constructions for the full action $\hat{S}^{\varepsilon}[\cdot]$ that have these interfaces as their zero level sets.

In one space dimension, it is straightforward to solve the limit problem posed by (2.3), but the reduced functional in $d > 1$ is more complicated to analyze. Below, we use it to develop two very different classes of candidates for upper bound constructions in $d > 1$, both of which give the same scaling law. The first class consists of one-dimensional constructions. The second class contains the MCF-based constructions, built around the mean-curvature-flow skeleton of Section 2. We emphasize that we do not claim to have found the optimal upper bound on the higher-dimensional action. What we have done is to develop and compare two classes of test functions. As always, the action cost of the constructions gives an upper bound on the action, but we do not expect the bound to be tight.

In some sense, it is surprising that one-dimensional constructions can compete with MCF-based constructions, which take advantage of the geometric freedom and deterministic dynamics associated with higher dimensions. Indeed, in Section 3.2, we show that at least for $d = 2$, accelerated mean-curvature flow can beat the one-dimensional constructions. In other words, in the part of parameter space in which accelerated MCF beat the one-dimensional constructions, action minimizers *must* involve two-dimensional structure. We expect that the behavior is generic for any $d \geq 2$; namely, that while one-dimensional constructions can achieve the optimal action in the energy-barrier regime, higher-dimensional constructions are necessary in the sharp-interface limit.

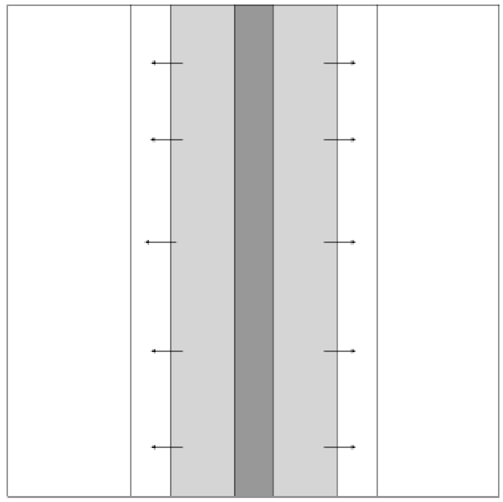

FIGURE 3.2. The stripe pattern, a one-dimensional construction for periodic boundary conditions.

If we assume that the action-minimizing front is monotone, we can rewrite the second term in (1.12) in terms of $\phi(x)$, the arrival time of the front at position x:

$$\frac{c_0}{4}\int_\Omega |\nabla\phi|\left(\frac{1}{|\nabla\phi|} + \nabla\cdot\frac{\nabla\phi}{|\nabla\phi|}\right)^2 dx. \tag{3.3}$$

Using (1.12) or (3.3) to study the full problem is in some sense the opposite of a current method in image processing, in which a sharp-interface problem is analyzed by studying a diffuse-interface approximation. See, for instance, [3, 6, 11].

One-Dimensional Constructions

PROPOSITION 3.4 (Upper Bound, One-Dimensional Constructions) *For periodic boundary conditions and $d > 1$, the action satisfies*

$$\limsup_{\varepsilon\to 0} \hat{S}_{\text{switch}} \le \min_{N\in\mathbb{N}}\left(2N + \frac{L^2}{8NT}\right)c_0\, L^{d-1}. \tag{3.4}$$

PROOF: We use the same construction as for $d = 1$, replacing the nucleation points with $(d-1)$–dimensional hyperplanes (which propagate as traveling planes). □

COROLLARY 3.5 *For Neumann boundary conditions and $d > 1$,*

$$\limsup_{\varepsilon\to 0} \hat{S}_{\text{switch}} \le \min_{N\in\mathbb{N}}\left(N + \frac{L^2}{4NT}\right)c_0 L^{d-1}.$$

Connection with Curvature Flow

The reduced action functional (2.1) suggests curvature flow. Indeed, as the sharp-interface analogue of (1.16), consider constructions of interface functions that are built out of point nucleations plus reverse and forward curvature flow to an intermediate state on the ridge, i.e., $\Gamma(T^*) = g$ and

$$v_n = \begin{cases} +\kappa, & 0 \le t \le T^*, \\ -\kappa, & T^* < t \le T. \end{cases} \tag{3.5}$$

Point nucleations incur no nucleation cost. Moreover, the calculation

$$\begin{aligned} S^R[\Gamma(\cdot)] &\ge \frac{c_0}{4} \int_0^{T^*} \int\limits_{\Gamma(t)} \big((v_n - \kappa)^2 + 4\,\kappa\, v_n\big) d\sigma\, dt \\ &\ge \frac{c_0}{4} \int_0^{T^*} \int\limits_{\Gamma(t)} (4\kappa v_n) d\sigma\, dt \\ &= \frac{c_0}{4} \int_0^{T^*} 4\dot{P}(\Gamma(t)) dt \\ &= c_0 P(g) \end{aligned}$$

shows that (3.5) — which leads to an action cost that is equal to c_0 times the perimeter of g — is the least possible action for any construction passing through g. This suggests the time-dependent perimeter problem:

> *What is the state with minimal perimeter that can be reached by forward and reverse curvature flow in time $T/2$?*

Note that we have not actually reduced the action minimization problem to a perimeter problem, because we have only demonstrated optimality among states that can be reached, in time, by curvature flow. In all likelihood, the optimal path accelerates or otherwise modifies its motion so that it can pass through an energetically better state in exchange for a nonzero propagation cost. These ideas generate the MCF-based upper bound constructions and accelerated MCF constructions below.

MCF-Based Constructions

For MCF-based constructions, we choose g to be a "checkerboard state" of appropriate scale and apply (3.5), as illustrated in Figure 3.3. The interfaces $\Gamma(t)$ serve as the zero level sets of the constructions.

PROPOSITION 3.6 (Upper Bound via MCF-Based Constructions) *For periodic boundary conditions and $d > 1$, there is a construction based on MCF whose*

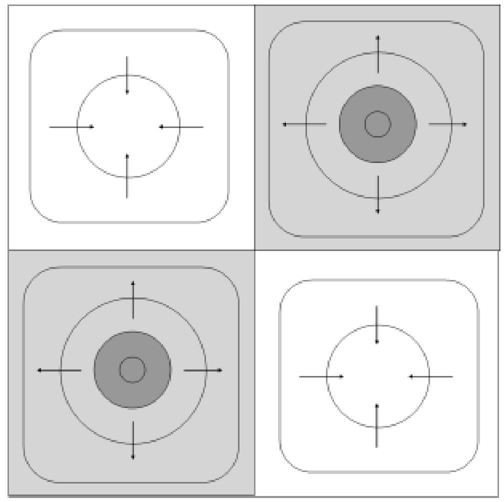

FIGURE 3.3. Sketch of an MCF construction. Reverse curvature motion carries the interface from two point nucleations to two gray squares. After the checkerboard is complete, the white squares collapse by forward curvature flow.

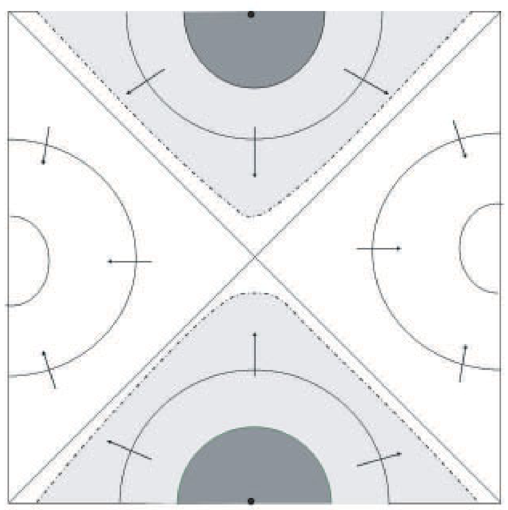

FIGURE 3.4. The cross pattern, an MCF construction for periodic boundary conditions.

limiting action cost (as $\varepsilon \to 0$) is exactly equal to the maximum over $t \in [0, T]$ of the perimeter of its zero level set. It satisfies the scaling

$$\limsup_{\varepsilon \to 0} \hat{S}^\varepsilon[u_\varepsilon] \lesssim \frac{L^d}{\sqrt{T}}. \tag{3.6}$$

Remark 3.7. By Proposition 4.1 below, (3.6) reflects the optimal scaling.

PROOF: We build the construction. The backbone is the interface, $\Gamma(t)$, which will define the zero level set of our test functions

$$u_\varepsilon(x, t) := \tanh\left(\frac{d(x, \Gamma(t))}{\varepsilon\sqrt{2}}\right). \tag{3.7}$$

We create the interface at time $0 < t' \ll 1$, with $\Gamma(t')$ a finite collection of points. We need to connect $u_\varepsilon(x, t')$ to the initial state $u_\varepsilon(x, 0) \equiv -1$ and count the action on $[0, t']$ separately. However, since $\Gamma(t')$ is comprised of only finitely many points,

$$\hat{E}^\varepsilon[u_\varepsilon(\,\cdot\,, t')] \underset{\varepsilon \to 0}{\to} 0,$$

and consequently we can connect the states with negligible action cost.

Let ℓ be the largest possible value such that $[0, \ell]^d$ collapses by MCF in time $t = T/2$. (The length scale ℓ scales like $\sqrt{T}$.) Since we are only interested in the scaling, we assume for simplicity that $L/\ell \in \mathbb{N}$. To construct $\Gamma(t)$, break the system into $n = (L/\ell)^d$ periodic cells so that on each cell, there is sufficient time to follow the reverse MCF path from a point to a square. To proceed, consider a checkerboard overlay of the system. A four-square checkerboard is sketched in Figure 3.3. On the black squares, let $\Gamma(0)$ be the center of the square, and $\Gamma(T/2)$ be the perimeter of the square. For $t \in [0, T/2]$, let the interface move by reverse mean-curvature flow from the initial to final state. Thus, at $t = T/2$, the interface has grown to the outline of the checkerboard. For $t \in [T/2, T]$, let the interface relax from this state to the centers of the white squares by forward curvature motion.

Since we use the deterministic motion, the limiting action cost is just the perimeter of the "checkerboard state" with n cells (cf. Section 3.2):

$$\lim_{\varepsilon \to 0} \hat{S}^\varepsilon[u_\varepsilon] = c_0 P = \frac{d c_0 L^d}{\ell} \sim \frac{L^d}{\sqrt{T}}.$$

□

Remark 3.8. Under periodic boundary conditions, the smallest checkerboard reduces to a cross pattern (Figure 3.4), where two point nucleations at a pair of parallel edges introduce growing interfaces. Since the energy barrier of the cross is higher than that of the one-dimensional stripe, the stripe achieves a lower action than the cross in the energy barrier regime. In the sharp-interface limit, however, curvature-based constructions are competitive; see below.

Remark 3.9. Our checkerboard construction "is in no hurry." If the interface were to move faster than the natural timescale, it could go through a coarser, energetically favored checkerboard at the expense of a propagation cost. We use this idea in the following proposition for dimension $d = 2$.

Accelerated Curvature Flow

In $d = 2$, we know the precise timescale for curvature motion. We use this information to show that accelerated curvature flow (checkerboards with $v_n = \gamma\kappa$ for $\gamma > 1$) can beat one-dimensional constructions in the sharp-interface regime. We do not claim that this is the optimal construction, but it shows that the optimal path must have two-dimensional structure. (This is *not* true in the energy-barrier regime; cf. Appendix A.)

PROPOSITION 3.10 (Upper Bound, $d = 2$, Accelerated MCF) *For periodic boundary conditions and dimension $d = 2$, the action satisfies*

$$\limsup_{\varepsilon\to 0} \hat{S}_{\text{switch}} \le \min_{N\in\mathbb{N}} \left(\frac{(2N)^3 \pi\, T}{L^2} + \frac{L^2}{2N\pi T} \right) c_0 L. \tag{3.8}$$

PROOF: The proof is by construction of an upper bound, and we again use the form (3.7) and need only specify the interface, $\Gamma(t)$. We use an $N \times N$ checkerboard as in the previous proposition. Let the normal velocity of the interface on any given square be a constant multiple of the curvature, $v_n = \pm\gamma\kappa$ for some $\gamma > 0$. We will choose the constant $\gamma = \gamma(N)$ so that the checkerboard is reached in exactly time $T/2$. For any closed, planar curve,

$$\dot{A}(t) = \int\limits_{\Gamma(t)} v_n = -\int\limits_{\Gamma(t)} \gamma\kappa = -\gamma \int\limits_{\Gamma(t)} \frac{d\theta}{d\sigma}\, d\sigma = -2\pi\gamma,$$

where $A(t)$ is the area enclosed by the curve $\Gamma(t)$ and θ is the angle between a point on the curve and a fixed axis. Therefore, we impose

$$\ell^2 = \pi\gamma T \Rightarrow \gamma = \frac{\ell^2}{\pi T} = \frac{L^2}{\pi T N^2}. \tag{3.9}$$

We calculate the cost in the reduced action functional for the growth phase:

$$\begin{aligned}
\frac{c_0}{4} \int_0^{T/2} \int\limits_{\Gamma(t)} (v_n + \kappa)^2 d\sigma\, dt &= \frac{c_0}{4} (1+\gamma)^2 \int_0^{T/2} \int\limits_{\Gamma(t)} \kappa^2\, d\sigma\, dt \\
&= \frac{c_0}{4} \frac{(1+\gamma)^2}{\gamma} \int_0^{T/2} \int\limits_{\Gamma(t)} \kappa v_n\, d\sigma\, dt \\
&= \frac{c_0}{4} \frac{(1+\gamma)^2}{\gamma} P\left(\frac{T}{2}\right) \\
&= \frac{c_0}{4} \frac{(1+\gamma)^2}{\gamma} 2NL,
\end{aligned}$$

and similarly for the collapse phase:

$$\frac{c_0}{4}\int_{T/2}^{T}\int\limits_{\Gamma(t)}(v_n+\kappa)^2\,d\sigma\,dt=\frac{c_0}{4}\,\frac{(1-\gamma)^2}{\gamma}\,2NL.$$

(In particular, choosing $v_n=\kappa$ accrues no cost for the collapse phase. The optimal n typically requires $\gamma>1$, however, since that allows for a smaller perimeter.) Adding the costs, substituting for γ from (3.9), and keeping in mind the periodicity requirement leads to (3.8). □

If we minimize over $N\in\mathbb{R}$, we find that the action for the MCF constructions does slightly better (by a factor of 0.99) than the one-dimensional constructions. It also does better when minimizing over integers for a wide range of the parameter $L/\sqrt{T}$. Proposition 3.10 implies that action minimizers must be fully two-dimensional in $d=2$ in any region of (L,T)–parameter space in which the minimum on the right-hand side of (3.8) is less than that on the right-hand side of (3.4). It does not imply the converse, however: when the right-hand side of (3.4) is less, there may still be another type of two-dimensional construction that does better. The optimal upper bound and the crossover point between one-dimensional and higher-dimensional minimizers are open questions.

4 Lower Bounds

After developing upper bounds via constructions, the goal is to develop matching, ansatz-free lower bounds which prove that no other construction can do better. We begin by developing the rough lower bound $\hat{S}_{\text{switch}}\geq L^d/(3\sqrt{T})$ for arbitrary dimension. This shows that the bounds proven in Propositions 3.1, 3.6, and 3.10 are optimal in terms of scaling. An ansatz-free, tight lower bound requires more work and relies on the limiting behavior of the energy measures. In Section 4.2, we illustrate the role of the energy by demonstrating how two hypotheses on the energy (reasonable for action minimizers) and an elementary argument lead to the improved one-dimensional lower bound

$$\liminf_{\varepsilon\to 0}\hat{S}_{\text{switch}}\geq c_0\frac{L}{\sqrt{T}}. \tag{4.1}$$

This bound is sharp (i.e., it matches the upper bound) when $L/(4\sqrt{T})\in\mathbb{N}$. In Section 4.3, we consider what is necessary for a rigorous proof.

4.1 Scaling Bound

PROPOSITION 4.1 (Lower Bound Scaling) *For all functions u with*

$$u(x,0)\equiv -1 \quad \textit{and} \quad u(x,T)\equiv +1$$

(*with periodic or Neumann boundary conditions*), *the action functional satisfies*

$$\hat{S}^{\varepsilon}[u]\geq\frac{1}{3}\,\frac{L^d}{\sqrt{T}}.$$

PROOF: On the one hand, letting $E(t) := \hat{E}^\varepsilon[u(\,\cdot\,,t)]$,

$$\hat{S}^\varepsilon[u] \geq \max_{0\leq t\leq T} E(t) \geq \frac{1}{T}\int_0^T E(t)dt \geq \frac{1}{T}\int_0^T \int\limits_{\Omega_L} \frac{(1-u^2)^2}{4\varepsilon}\,dx\,dt. \tag{4.2}$$

On the other hand,

$$\hat{S}^\varepsilon[u] \geq \frac{1}{4}\int_0^T \int\limits_{\Omega_L} \varepsilon\dot{u}^2\,dx\,dt.$$

Combining these inequalities,

$$\begin{aligned}
\hat{S}^\varepsilon[u] &\geq \frac{1}{2}\left(\frac{1}{4}\int_0^T \int\limits_{\Omega_L} \varepsilon\dot{u}^2\,dx\,dt + \frac{1}{T}\int_0^T \int\limits_{\Omega_L} \frac{(1-u^2)^2}{4\varepsilon}\,dx\,dt\right)\\
&\geq \frac{1}{4}\left(\int_0^T \int\limits_{\Omega_L} \dot{u}^2\,dx\,dt\right)^{1/2}\left(\frac{1}{T}\int_0^T \int\limits_{\Omega_L} (1-u^2)^2\,dx\,dt\right)^{1/2}\\
&\geq \frac{1}{4\sqrt{T}}\int_0^T \int\limits_{\Omega_L} |\dot{u}(1-u^2)|dx\,dt\\
&= \frac{1}{4\sqrt{T}}\int\limits_{\Omega_L}\int_0^T |\dot{u}(1-u^2)|dt\,dx\\
&\geq \frac{L^d}{3\sqrt{T}}.
\end{aligned}$$

□

4.2 Sharp One-Dimensional Bound under Two Assumptions

We derive the improved bound (4.1) under two hypotheses: aside from a small initial and final layer in time, the energy is approximately constant, and there is "approximate equipartition of energy" in the sense of (4.4) below. The hypotheses are natural in dimension one: To achieve switching, the function *must* form interfaces, and since there is no advantage for walls to nucleate late or disappear early, we expect the number of walls to remain fixed. Moreover, the $D_u\hat{E}^\varepsilon$ term in (1.10) drives the interfaces towards the optimal profile. Thus, in one dimension, we expect an approximately constant energy and approximate equipartition as the walls propagate.

PROPOSITION 4.2 (Tight Lower Bound with Assumptions) *Let the sequence of smooth functions $u_\varepsilon : [0, L] \to \mathbb{R}$ satisfy periodic or Neumann boundary conditions and $u_\varepsilon(x, 0) \equiv -1$ and $u_\varepsilon(x, T) \equiv +1$. Suppose that the following two assumptions also hold as $\varepsilon \to 0$:*

(i) *There are times $T' = o(1)$, $T'' = T - o(1)$, such that*

$$E(T') = E(T'') = \max_{0\le t\le T} E(T) + o(1). \tag{4.3}$$

(ii) *On $[T', T'']$, we have approximate equipartition of energy, i.e.,*

$$\frac{1}{2}\int_{\Omega_L} \varepsilon (u_{\varepsilon,x})^2\,dx = \int_{\Omega_L} \frac{V(u_\varepsilon)}{\varepsilon}\,dx + o(1). \tag{4.4}$$

Then

$$\liminf_{\varepsilon\to 0} \hat{S}^\varepsilon[u_\varepsilon] \ge c_0 \frac{L}{\sqrt{T}}.$$

PROOF: Taking the limit on the sequence is necessary only to remove the $o(1)$ terms. Therefore, in the following calculations, we fix ε and omit the subscript on the function u. Define

$$E_{\max} := \max_{0\le t\le T} E(t).$$

We split the action over $[0, T']$ and $[T', T'']$. On the first interval, there is a nucleation cost that comes from the jump in energy:

$$\hat{S}^\varepsilon_{[0,T']}[u] \ge E_{\max} + o(1). \tag{4.5}$$

On the second interval, there is a propagation cost from the motion of the interfaces. To estimate the cost, we introduce the following lemma:

LEMMA 4.3 (Control in Time) *Let*

$$I(t) := \int_0^L \left(u - \frac{u^3}{3}\right)(\,\cdot\,, t)dx.$$

We have the estimate

$$|I(t) - I(s)| \le C|t-s|^{1/2}.$$

PROOF: We combine the action and energy bounds

$$\begin{aligned} |I(t) - I(s)| &= \left| \int_s^t \int_0^L \dot{u}(1-u^2)dx\,dt' \right| \\ &\le \left(\int_s^t \int_0^L \varepsilon \dot{u}^2\,dx\,dt' \right)^{1/2} \left(\int_s^t \int_0^L \frac{(1-u^2)^2}{\varepsilon}\,dx\,dt' \right)^{1/2} \\ &\le C|t-s|^{1/2}. \end{aligned}$$

□

Lemma 4.3 and the initial and final conditions imply

$$J := \int_{T'}^{T''} \int_0^L \dot{u}(1-u^2)dx\,dt = \frac{4}{3}L + o(1). \tag{4.6}$$

On the other hand,

$$J \le \left(\int_{T'}^{T''} \int_0^L \varepsilon \dot{u}^2 \, dx \, dt \right)^{1/2} \left(\int_{T'}^{T''} \int_0^L \frac{(1-u^2)^2}{\varepsilon} \, dx \, dt \right)^{1/2}.$$

The idea is to use the $\iint \varepsilon \dot{u}^2 \, dx \, dt$ term to estimate the propagation cost. We have

$$\begin{aligned} &\frac{1}{4} \int_{T'}^{T''} \int_0^L \left(\varepsilon^{1/2} \dot{u} + \varepsilon^{-1/2} D_u \hat{E}^\varepsilon(u) \right)^2 dx \, dt \\ &= \frac{1}{4} \int_{T'}^{T''} \int_0^L \varepsilon \dot{u}^2 + \varepsilon^{-1} D_u \hat{E}^\varepsilon(u)^2 \, dx \, dt + \frac{1}{2}(E(T'') - E(T')) \\ &\ge \frac{1}{4} \int_{T'}^{T''} \int_0^L \varepsilon \dot{u}^2 \, dx \, dt, \end{aligned}$$

where the energy difference vanishes, by (4.3). Therefore,

$$\begin{aligned} J &\le 2(S_{[T',T'']}[u])^{1/2} \left(\int_{T'}^{T''} \int_0^L \frac{(1-u^2)^2}{\varepsilon} \, dx \, dt \right)^{1/2} \\ &\overset{(4.4)}{\le} 2(S_{[T',T'']}[u])^{1/2} \left(2 \int_{T'}^{T''} E(t) + o(1) dt \right)^{1/2} \\ &\le 2\sqrt{2T} (S_{[T',T'']}[u])^{1/2} (E_{\max} + o(1))^{1/2}. \end{aligned} \tag{4.7}$$

Combining (4.6) and (4.7),

$$S_{[T',T'']}[u] \ge \frac{2}{9} \frac{L^2}{T E_{\max}} + o(1). \tag{4.8}$$

Thus, from (4.5) and (4.8) we conclude

$$\begin{aligned} S[u] &\ge \min_M \left(M + \frac{2}{9} \frac{L^2}{TM} \right) + o(1) \\ &\ge \frac{2\sqrt{2}}{3} \frac{L}{\sqrt{T}} + o(1). \end{aligned}$$

Taking the limit on the sequence of functions completes the proof. □

4.3 Ansatz-Free Bounds and Equipartition of Energy

A rigorous proof requires an analysis of the weak convergence of the energy measures and the limiting equipartition of energy. This is related to work of Hutchinson and Tonegawa [20] and Tonegawa [37], who study energy-bounded sequences for which

$$f_\varepsilon := \varepsilon \Delta u_\varepsilon + \varepsilon^{-1}(u_\varepsilon - u_\varepsilon^3) \tag{4.9}$$

is a bounded sequence of constants, or a sequence of functions that is bounded in $W^{1,d}$. They prove that the density of the limiting energy measures has integer multiplicity almost everywhere (modulo c_0), and equipartition of energy is achieved in the limit.

The analytical challenge in our setting is to extend these results under the weaker bound

$$\varepsilon^{-1} \int_0^T \int_\Omega f_\varepsilon^2 \, dx \, dt \leq C. \tag{4.10}$$

The one-dimensional case is treated in [22]. It is shown that for action-bounded sequences, the energy measures

$$\left(\frac{\varepsilon u_{\varepsilon,x}^2}{2} + \frac{V(u_\varepsilon)}{\varepsilon} \right) dx \, dt$$

converge for all but possibly finitely many times to sums of delta masses whose coefficients are integers (modulo c_0). Using the convergence of the energy measures, their result (reformulated for periodic boundary conditions and spatial domain $[0, L]$) states

$$\liminf_{\varepsilon \to 0} S_\varepsilon[u_\varepsilon] \geq c_0 \min_{N \in \mathbb{Z}^+} \left(2N + \frac{L^2}{8NT} \right).$$

In other words, the upper bound in Proposition 3.1 is optimal. Moreover, they show that under the assumption that all interfaces are "simple" (i.e., have energy $1 \times c_0$), the action is bounded below by the reduced functional (1.13). (For a precise statement, see [22, theorem 1.4]).

In this subsection, our goal is to demonstrate that the key ingredients for the lower bound on the action functional in *any dimension* are the convergence of the energy measures and the limiting equipartition of energy. We show that provided the interface of the limit function, $\Gamma(t) := \partial\{u_0 = 1\}$, is sufficiently smooth and we have

(1) convergence of the energy measures with "single multiplicity"

$$\left(\frac{\varepsilon |\nabla u_\varepsilon|^2}{2} + \frac{V(u_\varepsilon)}{\varepsilon} \right) dx \, dt \rightharpoonup c_0 \mathcal{H}^{(d-1)} \llcorner \Gamma(t) dt =: \mu, \tag{4.11}$$

(2) limiting equipartition of energy, or vanishing of the discrepancy measures,

$$\left| \frac{\varepsilon |\nabla u_\varepsilon|^2}{2} - \frac{V(u_\varepsilon)}{\varepsilon} \right| dx \, dt \rightharpoonup 0, \tag{4.12}$$

then we have lower semicontinuity of the action functional in the sense that

$$\liminf_{\varepsilon\to 0}\int_0^T\int_\Omega \varepsilon\dot u_\varepsilon^2\,dx\,dt \ge c_0\int_0^T\int_{\Gamma(t)} v_n^2\,d\sigma\,dt, \tag{4.13}$$

$$\liminf_{\varepsilon\to 0}\int_0^T\int_\Omega \varepsilon^{-1}(\varepsilon\Delta u_\varepsilon-\varepsilon^{-1}V'(u_\varepsilon))^2\,dx\,dt \ge c_0\int_0^T\int_{\Gamma(t)} \kappa^2\,d\sigma\,dt. \tag{4.14}$$

We begin by showing (4.13). Let the set $\mathcal{A}$ consist of all $\zeta \in C_0^1(\Omega\times(0,T))$ such that

$$\int_0^T\int_{\Gamma(t)} \zeta^2\,d\sigma\,dt \le 1. \tag{4.15}$$

We will use the dual representation

$$\left(\int_0^T\int_{\Gamma(t)} v_n^2\,d\sigma\,dt\right)^{1/2} = \sup_{\zeta\in\mathcal{A}}\int_0^T\int_{\Gamma(t)} \zeta v_n\,d\sigma\,dt. \tag{4.16}$$

Let $A(t)$ denote the set $\{u_0=-1\}$ and take the sign convention that v_n is the normal velocity in the direction of the *outward* normal to A. We have two equalities:

$$\int_0^T\int_{\Gamma(t)} \zeta v_n\,d\sigma\,dt = -\int_0^T\int_{A(t)} \dot\zeta\,dx\,dt,$$

$$\int_0^T\int_{\Gamma(t)} \zeta v_n\,d\sigma\,dt = \int_0^T\int_{A^c(t)} \dot\zeta\,dx\,dt.$$

Combining the equalities,

$$\begin{aligned}
&\int_0^T\int_{\Gamma(t)} \zeta v_n\,d\sigma\,dt\\
&\quad= \frac12\left(-\int_0^T\int_{A(t)} \dot\zeta\,dx\,dt + \int_0^T\int_{A^c(t)} \dot\zeta\,dx\,dt\right)\\
&\quad= \frac34\liminf_{\varepsilon\to 0}\left(\int_0^T\int_\Omega \dot\zeta\left(u_\varepsilon-\frac{u_\varepsilon^3}{3}\right)dx\,dt\right)\\
&\quad= \frac34\liminf_{\varepsilon\to 0}\left(-\int_0^T\int_\Omega \zeta\dot u_\varepsilon(1-u_\varepsilon^2)\,dx\,dt\right)\\
&\quad\le \frac34\liminf_{\varepsilon\to 0}\left(\int_0^T\int_\Omega \zeta^2\frac{(1-u_\varepsilon^2)^2}{\varepsilon}\,dx\,dt\right)^{1/2}\left(\int_0^T\int_\Omega \varepsilon\dot u_\varepsilon^2\,dx\,dt\right)^{1/2}
\end{aligned}$$

$$\overset{(4.11)}{\underset{(4.12)}{=}} \frac{3}{4}\left(2c_0\int_0^T\int_{\Gamma(t)} \zeta^2\,d\sigma\,dt\right)^{1/2}\liminf_{\varepsilon\to 0}\left(\int_0^T\int_\Omega \varepsilon\dot{u}_\varepsilon^2\,dx\,dt\right)^{1/2}$$

$$\overset{(4.15)}{\le} c_0^{-1/2}\liminf_{\varepsilon\to 0}\left(\int_0^T\int_\Omega \varepsilon\dot{u}_\varepsilon^2\,dx\,dt\right)^{1/2}.$$

By the representation (4.16), taking the sup over ζ implies (4.13).

Similarly, to show (4.14), we let the set $\mathcal{A}$ consist of all $\xi \in C_0^1(\Omega\times(0,T))^d$ such that

$$\int_0^T\int_{\Gamma(t)} |\xi|^2\,d\sigma\,dt \le 1 \tag{4.17}$$

and use the dual representation

$$\left(\int_0^T\int_{\Gamma(t)} |\underline{\kappa}|^2\,d\sigma\,dt\right)^{1/2} = \sup_{\xi\in\mathcal{A}}\int_0^T\int_{\Gamma(t)} (\xi\cdot\underline{\kappa})d\sigma\,dt, \tag{4.18}$$

where $\underline{\kappa}$ is the mean-curvature vector.

First, we claim that (i) and (ii) imply

$$\begin{aligned}
&\int_0^T\int_\Omega\left(\nabla\cdot\xi - \partial_i\xi_j\frac{\partial_i u_\varepsilon}{|\nabla u_\varepsilon|}\frac{\partial_j u_\varepsilon}{|\nabla u_\varepsilon|}\right)\varepsilon|\nabla u_\varepsilon|^2\,dx\,dt\\
&\qquad\to c_0\int_0^T\int_{\Gamma(t)}\big(\nabla\cdot\xi - \partial_i\xi_j\,\nu_i\otimes\nu_j\big)d\sigma\,dt\\
&\qquad= c_0\int_0^T\int_{\Gamma(t)}(\xi\cdot\underline{\kappa})d\sigma\,dt.
\end{aligned}\tag{4.19}$$

(We use a summation convention, and ν denotes the outward unit normal to the region enclosed by $\Gamma(t)$.) The convergence of the first term is a direct application of (i) and (ii). The convergence of the second term relies on the following consequence of conditions (i) and (ii), which follows from work of Reshetnyak [31]; see also Luckhaus and Modica [25]. Their results are more general; in our setting, the statement we need is the following:

PROPOSITION 4.4 *Suppose conditions* (i) *and* (ii) *are satisfied. Then*

$$\varepsilon\nabla u_\varepsilon\otimes\nabla u_\varepsilon\,dx\,dt \rightharpoonup c_0\nu\otimes\nu\mathcal{H}^{(d-1)}\llcorner\Gamma(t)dt.$$

For completeness, we include the proof.

PROOF: Because

$$\lambda_\varepsilon := \varepsilon\nabla u_\varepsilon\otimes\nabla u_\varepsilon\,dx\,dt$$

is a bounded sequence of measures, we may assume without loss that it converges to a limit measure λ. Moreover, (4.12) implies that the limiting measure μ (defined in (4.11)) is equal to

$$\mu = \lim_{\varepsilon\to 0} \varepsilon|\nabla u_\varepsilon|^2 \, dx \, dt.$$

Therefore, $|\lambda| \ll \mu$ and by the Radon-Nikodym theorem, it has a representation

$$\lambda = B\mu$$

for some μ-measurable matrix B that is symmetric and positive semidefinite.

We now study the matrix B. All of the statements that we make about B should be understood in the μ-a.e. sense.

First of all, the calculation

$$\mu = \lim_{\varepsilon\to 0} \varepsilon|\nabla u_\varepsilon|^2 \, dx \, dt = \lim_{\varepsilon\to 0} \operatorname{Tr}(\varepsilon \nabla u_\varepsilon \otimes \nabla u_\varepsilon) dx \, dt = \operatorname{Tr}(B)\mu$$

reveals that

$$\operatorname{Tr} B = 1, \tag{4.20}$$

which by the positivity of B implies in particular that the maximal eigenvalue of B is bounded by 1. Thus

$$(y, By) \le 1 \tag{4.21}$$

for any $y \in \mathbb{R}^d$ with $|y| \le 1$. The goal is now to show that

$$(\nu, B\nu) = 1 \quad \mu\text{-a.e.}, \tag{4.22}$$

which by the Rayleigh quotient implies that ν is an eigenvector of B with eigenvalue 1. Because of (4.20) and the positivity of B, ν must therefore be the *only* eigenvector of B with nontrivial eigenvalue, and $B = \nu \otimes \nu$.

For the proof of (4.22), let $\xi \in C_0^\infty(\Omega \times (0, T))^d$ with $|\xi| \le 1$ and observe:

$$\begin{aligned}
\varepsilon(\xi, \nabla u_\varepsilon \otimes \nabla u_\varepsilon \xi) = \varepsilon(\nabla u_\varepsilon, \xi)^2 &= \varepsilon|\nabla u_\varepsilon|^2 \left(\frac{\nabla u_\varepsilon}{|\nabla u_\varepsilon|}, \xi \right)^2 \\
&\ge \varepsilon|\nabla u_\varepsilon|^2 \left(2\left(\frac{\nabla u_\varepsilon}{|\nabla u_\varepsilon|}, \xi \right) - 1 \right) \\
&= 2\varepsilon|\nabla u_\varepsilon|(\nabla u_\varepsilon, \xi) - \varepsilon|\nabla u_\varepsilon|^2, \qquad (4.23)
\end{aligned}$$

where to get to the second line, we have used the inequality $x^2 \ge 2x - 1$.

We would like to integrate and pass to the limit in (4.23). The difficult term is the first term on the right-hand side. For this term, we will use the fact that for all ξ with $|\xi| \le 1$,

$$\begin{aligned}
&\iint \big|2\varepsilon|\nabla u_\varepsilon|(\nabla u_\varepsilon,\xi)-\sqrt{2}|1-u_\varepsilon^2|(\nabla u_\varepsilon,\xi)\big|dx\,dt\\
&=\iint \big|2\varepsilon|\nabla u_\varepsilon|^2-\sqrt{2}|1-u_\varepsilon^2|\,|\nabla u_\varepsilon|\big|\left|\left(\frac{\nabla u_\varepsilon}{|\nabla u_\varepsilon|},\xi\right)\right|dx\,dt\\
&\le \iint \big|2\varepsilon|\nabla u_\varepsilon|^2-\sqrt{2}|1-u_\varepsilon^2|\,|\nabla u_\varepsilon|\big|\,dx\,dt\\
&\le \left(\iint \varepsilon|\nabla u_\varepsilon|^2\,dx\,dt\iint\left(2\sqrt{\varepsilon}|\nabla u_\varepsilon|-\sqrt{2}\,\frac{|1-u_\varepsilon^2|}{\sqrt{\varepsilon}}\right)^2dx\,dt\right)^{1/2}\\
&\le \left(\iint \varepsilon|\nabla u_\varepsilon|^2\,dx\,dt\iint\left|4\varepsilon|\nabla u_\varepsilon|^2-2\,\frac{(1-u_\varepsilon^2)^2}{\varepsilon}\right|dx\,dt\right)^{1/2}\\
&=2\sqrt{2}\left(\iint \varepsilon|\nabla u_\varepsilon|^2\,dx\,dt\iint\left|\frac{\varepsilon|\nabla u_\varepsilon|^2}{2}-\frac{V(u_\varepsilon)}{\varepsilon}\right|dx\,dt\right)^{1/2},
\end{aligned}$$

which goes to zero by (4.12). Therefore,

$$\begin{aligned}
&\lim_{\varepsilon\to 0}\int_0^T\int_\Omega 2\varepsilon|\nabla u_\varepsilon|(\nabla u_\varepsilon,\xi)\,dx\,dt\\
&\qquad=\lim_{\varepsilon\to 0}\int_0^T\int_\Omega \sqrt{2}\,|1-u_\varepsilon^2|(\nabla u_\varepsilon,\xi)\,dx\,dt.
\end{aligned}\tag{4.24}$$

Defining

$$W(u):=\int_0^u|1-s^2|\,ds,$$

(4.24) and the convergence of u_ε to ± 1 imply

$$\begin{aligned}
&\lim_{\varepsilon\to 0}\int_0^T\int_\Omega 2\varepsilon|\nabla u_\varepsilon|(\nabla u_\varepsilon,\xi)\,dx\,dt\\
&\quad=\lim_{\varepsilon\to 0}\int_0^T\int_\Omega \sqrt{2}\,(\nabla W(u_\varepsilon),\xi)\,dx\,dt\\
&\quad=\lim_{\varepsilon\to 0}\int_0^T\int_\Omega -\sqrt{2}\,W(u_\varepsilon)\,(\nabla\cdot\xi)\,dx\,dt\\
&\quad=c_0\int_0^T\int_{A(t)}(\nabla\cdot\xi)\,dt-\,c_0\int_0^T\int_{A^c(t)}(\nabla\cdot\xi)\,dt\\
&\quad=2c_0\int_0^T\int_{\Gamma(t)}(\xi,\nu)\,dt=2\int(\xi,\nu)d\mu.
\end{aligned}$$

Therefore, integrating and taking the limit in (4.23),

$$\int (\xi, B\xi) d\mu \geq 2 \int (\xi, \nu) d\mu - \int d\mu.$$

Letting ξ approximate ν, we conclude

$$\int (\nu, B\nu) d\mu \geq \int d\mu,$$

which, in light of (4.21), implies (4.22) and completes the proof. □

We will use (4.19) together with the following identity, which we derive by multiplying (4.9) by $\partial_j u_\varepsilon \xi_j$ and integrating by parts:

$$\begin{aligned} &\int_0^T \int_\Omega \left(\nabla \cdot \xi - \partial_i \xi_j \frac{\partial_i u_\varepsilon}{|\nabla u_\varepsilon|} \frac{\partial_j u_\varepsilon}{|\nabla u_\varepsilon|} \right) \varepsilon |\nabla u_\varepsilon|^2 \, dx \, dt \\ &= \int_0^T \int_\Omega \left((\nabla \cdot \xi) \left(\varepsilon \frac{|\nabla u_\varepsilon|^2}{2} - \frac{V(u_\varepsilon)}{\varepsilon} \right) + f_\varepsilon \partial_j u_\varepsilon \xi_j \right) dx \, dt. \end{aligned} \tag{4.25}$$

If the sum of the first two terms on the right-hand side vanishes in the limit by equipartition of energy (cf. (4.12)), then (4.19) and (4.25) imply

$$\begin{aligned} c_0 &\int_0^T \int_{\Gamma(t)} (\xi \cdot \underline{\kappa}) \, d\sigma \, dt \\ &= \liminf_{\varepsilon \to 0} \int_0^T \int_\Omega \left(\nabla \cdot \xi - \partial_i \xi_j \frac{\partial_i u_\varepsilon}{|\nabla u_\varepsilon|} \frac{\partial_j u_\varepsilon}{|\nabla u_\varepsilon|} \right) \varepsilon |\nabla u_\varepsilon|^2 \, dx \, dt \\ &= \liminf_{\varepsilon \to 0} \int_0^T \int_\Omega (f_\varepsilon \, \partial_j u_\varepsilon \xi_j) dx \, dt \\ &\leq \liminf_{\varepsilon \to 0} \left[\left(\varepsilon^{-1} \int_0^T \int_\Omega f_\varepsilon^2 \, dx \, dt \right)^{1/2} \left(\int_0^T \int_\Omega \varepsilon |\nabla u_\varepsilon|^2 \, |\xi|^2 \, dx \, dt \right)^{1/2} \right]. \end{aligned}$$

Using (4.11) and (4.17) to bound the limit of the second term, we conclude

$$c_0 \int_0^T \int_{\Gamma(t)} (\xi \cdot \underline{\kappa}) \, d\sigma \, dt \leq \liminf_{\varepsilon \to 0} \left(\varepsilon^{-1} \int_0^T \int_\Omega f_\varepsilon^2 \, dx \, dt \right)^{1/2} c_0^{1/2},$$

which, together with the representation (4.18), implies (4.14).

The task of justifying hypotheses (i) and (ii) in space dimension greater than one remains a challenging open problem. The topic is linked to a conjecture of De Giorgi, on which there has been recent progress in two and three space dimensions [1, 30].

5 Outlook

Relevance of Short-Time Switching Pathways. Because "long-time switching pathways" (e.g., single-nucleation pathways in the Allen-Cahn problem; see Appendix A.2) are the most likely pathways when switching is considered on its natural timescale, they receive a lot of attention. After all, on this timescale, other switching pathways are exponentially unlikely. On shorter timescales, however, different switching pathways may become relevant. In that case, estimating the probability of switching based on the long-time pathway gives a gross underestimate. This phenomenon appears, for instance, in the context of magnetic memory devices [23, 32].

Large Systems. As discussed in the introduction, the large system limit we study here is taken *after sending the noise strength to zero.* As an example of a very different limit, consider

$$\dot{u} = u_{xx} - V'(u) + \sqrt{2\gamma}\,\eta, \quad x \in [-L, L],$$

where V is an *unequal* double-well potential and η is a space-time white noise. Nucleation events are localized and the joint limit $\gamma \to 0$ with $L \sim \exp(c/\gamma)$ leads to multiple nucleation events that are *randomly* distributed in space and time [33].

Sharp-Interface Limit of the Stochastic Process. Is the limiting functional (2.3) actually the action functional for a well-defined stochastic process? Moreover, is this process the sharp-interface limit of the process defined by (1.4)? These questions involve permuting the order of the ε- and γ-limits. Partial progress in this direction is contained in [16].

Interpreting the limiting functional (2.1) for $d > 1$ in terms of an associated stochastic, sharp-interface problem is yet more involved, since there is also the regularization parameter λ to consider. We are not aware of work in this direction at this time.

Boundary Vortex Limit in Micromagnetics. The topic of action minimization and sharp-interface limits for stochastically perturbed partial differential equations is certainly not limited to the Allen-Cahn equation, nor is the sharp-interface limit the only interesting one. In micromagnetics, for example, one is interested in thermally activated switching of the magnetization. There is a regime — involving submicron-scale, soft thin films, commonly used for magnetoresistive memory devices — in which the magnetic behavior is dominated by "boundary vortices" [24, 28, 29]. We wonder whether thermally activated switching in this regime can be described by minimizing a suitable action involving the nucleation and motion of boundary vortices.

Appendix A: Two Other Action Regimes

In this appendix, we consider two more limiting regimes of the action (1.18): the short-time limit ($T \to 0$) and the energy barrier regime ($L, T \to \infty$ with

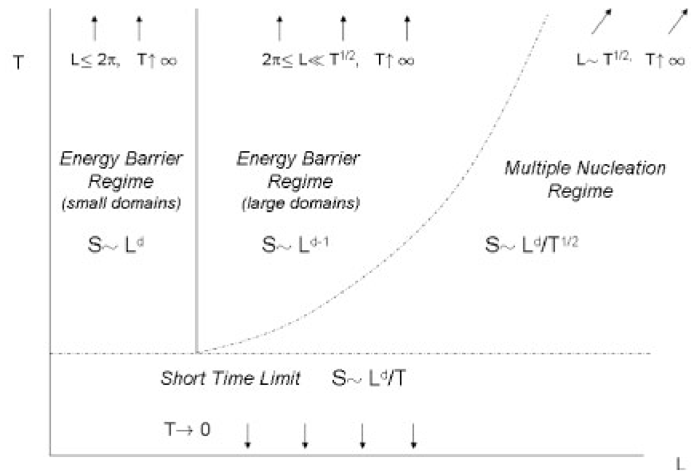

FIGURE A.1. The scaling of the action in the four-parameter regimes.

$L \ll \sqrt{T}$). See Figure A.1 for an overview. As usual, we focus on periodic boundary conditions, but suitable generalization to Dirichlet or Neumann boundary conditions is usually straightforward, as we remark.

A.1 Short-Time Limit

In the short-time limit ($T \to 0$),

$$S_{\text{switch}} \sim \frac{L^d}{T}.$$

The heuristic here is that because time is short, the transport term $\int_0^T \int_{\Omega_L} \dot{u}^2\,dx\,dt$ is paramount, leading us to expect spatial independence and, to minimize the transport term, linearity in time. We prove that such a path does indeed optimize the action. The short-time limit is unique in that the optimal path completely ignores the energy landscape.

PROPOSITION A.1 (Short-Time Limit) *For periodic or Neumann boundary conditions, the action satisfies*

$$\lim_{T \to 0} T\, S_{\text{switch}} = L^d.$$

PROOF: LOWER BOUND. We show that

$$S_{\text{switch}} \geq \frac{L^d}{T}.$$

We use the properties of the spatial mean, $\bar{u} := L^{-d} \int_{\Omega_L} u\,dx$, to bound the action from below. Note that $\bar{u}(t = 0) = -1$, $\bar{u}(t = T) = 1$, and

$$\inf_{\substack{\bar{u} \\ \bar{u}(0)=-1 \\ \bar{u}(T)=1}} \int_0^T \dot{\bar{u}}^2\,dt = \frac{4}{T}.$$

On the other hand, Jensen's inequality gives

$$\frac{1}{L^d} \int\limits_{\Omega_L} \dot{u}^2\,dx \geq \left(\frac{1}{L^d} \int\limits_{\Omega_L} \dot{u}\,dx \right)^2,$$

so that for any function u that switches in time T and obeys the boundary conditions,

$$\begin{aligned} S[u] &\geq \frac{1}{4} \int_0^T \int\limits_{\Omega_L} \dot{u}^2\,dx\,dt \\ &\geq \frac{L^d}{4} \int_0^T \dot{\bar{u}}^2\,dt \\ &\geq \frac{L^d}{T}. \end{aligned}$$

Taking the infimum over u completes the lower bound.

UPPER BOUND. We show that

$$\limsup_{T \to 0} T\,S_{\text{switch}} \leq L^d.$$

We choose $u := -1 + 2t/T$, the spatially independent linear interpolant between end states, as a test function and compute

$$\begin{aligned} \frac{1}{4} \int_0^T \int\limits_{\Omega_L} \dot{u}^2 + (\Delta u + u - u^3)^2\,dx\,dt &= \frac{L^d}{4} \int_0^T \frac{4}{T^2} + (u - u^3)^2\,dt \\ &= \frac{L^d}{T}(1 + O(T^2)). \end{aligned}$$

□

A.2 Energy-Barrier Regime

We now switch perspectives and consider the *long-time limit* of the action. Recall that the action is always at least as big as the energy barrier. The energy-barrier regime consists of the region of parameter space in which T is taken to infinity in such a way that this bound can be achieved. According to (1.16), an action-minimizing trajectory should follow the uphill gradient flow to the minimal saddle and the downhill flow from the saddle. Although infinite time is required to complete each of the uphill and downhill journeys along the heteroclinic orbits, a switching time that is large compared to the deterministic time scale allows a nearly optimal path to be constructed by modifying the flow near the critical points.

At first, one is surprised by the *extent* of the energy-barrier regime. The deterministic timescale for (1.3) in $d = 1$ is exponentially large in L; therefore, one might expect that the action is strictly larger than the energy barrier when $L \gg \ln T$. In fact, it is possible to achieve an action cost equal to the energy barrier in the limit $T \to \infty$ even when

$$\ln T \ll L \ll \sqrt{T}.$$

To achieve the bound, we use the same constructions as for the sharp-interface limit.

In $d > 1$, it seems natural that $L \sim \sqrt{T}$ marks the boundary of the energy barrier regime, since this is indeed the timescale for curvature flow. Even here, however, the sharp bound is surprising, since one-dimensional constructions are used to achieve the minimal action, and there is no apparent curvature-based construction that does as well.

There are two subregions of the energy barrier regime, distinguished by the uniformity or nonuniformity of the minimal saddle. The crossover is at $L = 2\pi$, at which point the saddle $u \equiv 0$ is supplanted by the nonuniform saddle. (The boundary condition affects the crossover point; for Neumann conditions, the transition is at $L = \pi$. For Dirichlet conditions, there is no small system regime, since there is only one critical point of the energy for $L < \pi$, and thus no switching problem.)

A.3 Energy Barrier Regime: Bounded Systems

For any bounded system, a long-time action bound equal to the energy barrier,

$$\lim_{T\to\infty} S_{\text{switch}} = \Delta E(L), \tag{A.1}$$

is achieved by an approximation of the pathway (1.16) through the minimal saddle. (Here $\Delta E(L)$ denotes the minimal saddle energy on an interval of length L.) For $L \le 2\pi$, the *only* saddle point is $u \equiv 0$ (cf. Appendix B.1). Thus, for $T \to \infty$ with $L \le 2\pi$,

$$\lim_{T\to\infty} S_{\text{switch}} = \frac{L^d}{4}.$$

For $L > 2\pi$, the minimal saddle is spatially nonuniform with an energy that scales like perimeter, so that

$$S_{\text{switch}} \sim L^{d-1}.$$

The convergence (A.1) follows from the elementary observation (1.15) combined with the construction of Faris and Jona-Lasinio ([13, theorem 9.1]). For completeness, we state the result:

PROPOSITION A.2 (Long-Time Limit, Bounded Systems) *For $L \in (0, \infty)$ and periodic boundary conditions, the action satisfies*

$$\lim_{T\to\infty} S_{\text{switch}} = \Delta E(L).$$

PROOF: LOWER BOUND. The lower bound comes from (1.15).

UPPER BOUND. As in the proof of Proposition 3.1, we construct a test function $\tilde{u}$ in five parts. The first is a linear interpolant connecting $u \equiv -1$ to a point arbitrarily nearby. The second follows the reversed dynamics to a point arbitrarily near the lowest energy saddle point. The third is a linear interpolant between that point and a point in the basin of attraction of $u \equiv +1$, also arbitrarily close to the saddle point. The fourth follows the gradient flow towards $u \equiv +1$. The fifth connects the endpoint of the fourth segment with $u \equiv +1$. By choosing T large enough, we can make the first, third, and fifth contributions to the action arbitrarily small, by Lemma 3.3. Thus,

$$\begin{aligned}\lim_{T\to\infty} S[\tilde{u}] &\le \frac{\delta}{3} + \Delta E(L) + \frac{\delta}{3} + 0 + \frac{\delta}{3}\\ &= \Delta E(L) + \delta.\end{aligned}$$

Letting $\delta \to 0$ completes the bound. □

Remark A.3. For $L \le 2\pi$, spatially uniform switching paths can be used to optimize the action, as in the short-time limit. Now it is the smallness of the length scale (rather than the timescale) that is responsible, however. The dynamics of the minimizing pathway are completely different from the temporally linear dynamics used for the short-time limit.

A.4 Energy Barrier Regime: Unbounded Systems

The action also scales like perimeter,

$$S_{\text{switch}} \sim L^{d-1},$$

for $L, T \to \infty$ with $L \ll \sqrt{T}$. To show it, we use the fact that we can actually calculate the limit of the energy barrier as $L \to \infty$ (Theorem B.5 in Appendix B) together with Propositions 3.1 and 3.4.

PROPOSITION A.4 *For $L, T \to \infty$ with $L/\sqrt{T} \to 0$, the action for periodic boundary conditions satisfies*

$$\lim_{\substack{L,T\to\infty\\ L/\sqrt{T}\to 0}} L^{1-d} S_{\text{switch}} = 2c_0. \tag{A.2}$$

PROOF:

Lower Bound. Turning once more to (1.15), we have that for all L and T,

$$L^{1-d}\Delta E(L) \le L^{1-d} S_{\text{switch}}. \tag{A.3}$$

Upper Bound. On the other hand, from Propositions 3.1 and 3.4,

$$\lim_{\substack{L,T\to\infty \\ L/\sqrt{T}\to 0}} L^{1-d} S_{\text{switch}} \leq 2c_0. \tag{A.4}$$

Moreover, by Theorem B.5 from Appendix B.3, we have

$$2c_0 = \lim_{L\to\infty} L^{1-d}\Delta E(L). \tag{A.5}$$

The combination of (A.3), (A.4), and (A.5) implies (A.2). □

Remark A.5. Proposition A.4 also holds for Neumann boundary conditions with $2c_0$ replaced by c_0.

Appendix B: The Energy and Its Saddle Points

The purpose of this appendix is to collect relevant information about the energy and its dependence on spatial scale. The energy barrier for small systems is derived in Corollary B.2 below, and the limit of the barrier for large systems is derived in Theorem B.5.

B.1 Small Systems

Small systems are particularly straightforward because the only periodic saddle point of the energy for $L < 2\pi$ is $u \equiv 0$. This fact follows from Theorem B.1 below, which is the adaptation to periodic boundary conditions of a theorem by Gurtin and Matano [18].

THEOREM B.1 *For $L < 2\pi$, the only periodic critical points are constant.*

PROOF: We use the fact that $-1 \leq u \leq 1$. (Suppose u has a maximum at x_0 with $u(x_0) > 1$. Then $\Delta u(x_0) \leq 0$ but $(u^3 - u)(x_0) > 0$. A similar contradiction rules out a minimum < -1.)

First, suppose u is a nonconstant critical point of one sign. Without loss, assume u is positive. Integrate the Euler-Lagrange equation, using the boundary condition to conclude

$$\int_{[0,L]^d} u(1-u^2)dx = 0. \tag{B.1}$$

Since the integrand is positive, it must vanish; thus $u \equiv 0$ or $u \equiv 1$. Similarly, if u is negative, $u \equiv 0$ or $u \equiv -1$.

Now suppose that u is a nonconstant critical point that changes sign. We will obtain a contradiction by the method of Gurtin and Matano. The idea is that we want to use the smallness of the spatial domain to invoke a Poincaré inequality that contradicts an inequality supplied by the equation. The problem is the mean value that appears in the Poincaré inequality. The method around it is the following.

Since u changes sign, we can define $w := u^+ + \alpha u^-$, with $\alpha > 0$ chosen such that $\int w = 0$. Furthermore, let $\tilde{w} := u^+ + \alpha^2 u^-$. Both w and $\tilde{w}$ are periodic. They also satisfy the relations

$$\begin{aligned} u\tilde{w} &= w^2, \\ \langle \nabla u, \nabla \tilde{w} \rangle &= |\nabla w|^2. \end{aligned} \tag{B.2}$$

Hence,

$$\begin{aligned} -\int_{[0,L]^d} \tilde{w}(u^3 - u)dx = -\int_{[0,L]^d} \tilde{w}\Delta u\, dx = \int_{[0,L]^d} \langle \nabla \tilde{w}, \nabla u \rangle\, dx \\ = \int_{[0,L]^d} |\nabla w|^2\, dx \geq \lambda \int_{[0,L]^d} w^2\, dx > \int_{[0,L]^d} w^2\, dx, \end{aligned}$$

where $\lambda = (2\pi/L)^2 > 1$ and no mean appears since by construction w has zero mean. On the other hand,

$$-\int_{[0,L]^d} \tilde{w}(u^3 - u)dx = -\int_{[0,L]^d} \tilde{w}u(u^2 - 1)dx \leq \int_{[0,L]^d} \tilde{w}u\, dx = \int_{[0,L]^d} w^2\, dx.$$

This contradiction establishes that there is in fact no nonconstant periodic critical point for $L < 2\pi$. □

COROLLARY B.2 *For $L < 2\pi$ and periodic boundary conditions, the only critical points of the energy $E[u] = \int_{[0,L]^d} \frac{1}{2}|\nabla u|^2 + \frac{1}{4}(1 - u^2)^2\, dx$ are $u \equiv \pm 1$ and $u \equiv 0$. The first two are minima*; *the last is a saddle point.*

Remark B.3. As discussed earlier, the transition for Dirichlet or Neumann boundary conditions is at $L = \pi$, and for Dirichlet conditions, there is no switching problem for small systems since there is only one critical point.

B.2 The Birth of a New Saddle Point

There is a sharp boundary at 2π demarcating the emergence of a new, lower energy saddle point that remains the minimal saddle for all $L \in (2\pi, \infty)$. The bifurcation is marked by the nontrivial nullspace of the linearization of the Euler-Lagrange equation about the zero solution. We begin with a calculation that is specific to one dimension. While we could proceed immediately with a theorem for arbitrary dimension, the one-dimensional case allows direct calculation and builds intuition. (As noted, the transition point for Dirichlet or Neumann conditions is instead at π.)

Consider the Euler-Lagrange equation

$$u_{xx} = V'(u),$$

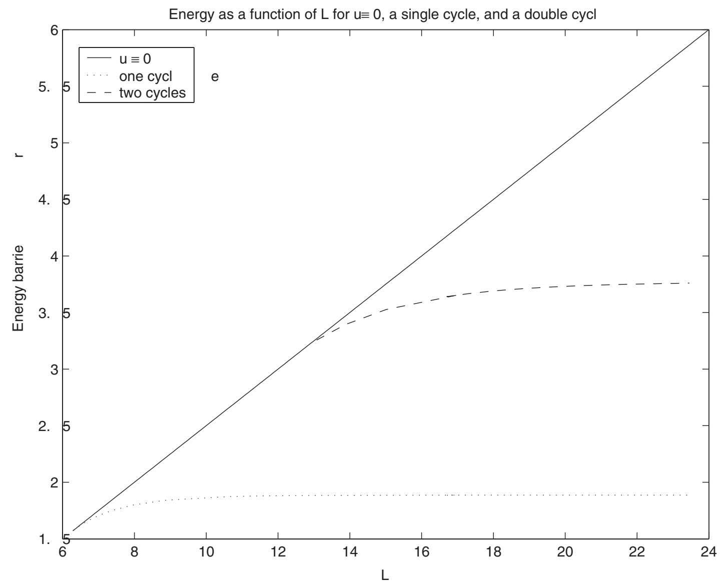

FIGURE B.1. The energy of the saddle points vs. L.

with $V(u) := (1-u^2)^2/4$. Recast it as a first-order system,

$$\begin{cases} u_x = p \\ p_x = V'(u), \end{cases} \tag{B.3}$$

a Hamiltonian system with Hamiltonian $H(u, p) := p^2/2 - V(u)$. L-periodic solutions of the system satisfy

$$L = 4\int_0^{u^*} \frac{du}{\sqrt{2(V(u) - V(u^*))}} =: f(u^*), \tag{B.4}$$

where u^* is the maximum value of u. The function $f(u^*)$ is monotonic increasing and

$$\lim_{u^* \to 0^+} f(u^*) = 2\pi.$$

For $L > 2\pi$, $f^{-1}(L)$ determines the unique maximum value u^*, assumed by u_L, the unique, nontrivial, single-cycle, L-periodic solution of (B.3). Then

$$E[u_L] = -HL + 4\int_0^{u^*} \sqrt{2(V(u) - V(u^*))}\, du \tag{B.5}$$

and $H = -V(u^*)$. We sample a range of u^* and use (B.4) and (B.5) to calculate the corresponding length and energy. Figure B.1 compares the energy as a function of L of the trivial solution, the nontrivial single-cycle saddle, and the nontrivial two-cycle solution.

As $L \to \infty$, $u^* \to 1$ and the minimal saddle converges to a "kink-antikink" pair of hyperbolic tangents. The energy converges to $4\sqrt{2}/3$, twice the cost of a domain wall. (For Neumann conditions, the convergence is to $2\sqrt{2}/3$, the cost of a single wall.)

Remark B.4. Note that in addition, for $L > 2n\pi$ for $n > 1$, there are $n - 1$ additional nontrivial solutions, corresponding to multiple cycles. These are higher-energy critical points, however. The energy of the 2-cycle saddle is illustrated in Figure B.1.

B.3 Bigger Systems in Higher Dimensions

In higher dimensions, it remains true that a nonuniform saddle emerges as the minimal saddle. We use an elementary method to calculate the limit of the minimal saddle point energy as $L \to \infty$ for periodic boundary conditions. (As in one dimension, the energy for Neumann conditions is half the value.)

THEOREM B.5 *We have*

$$L^{1-d} E[\textit{minimal saddle}] \underset{L\to\infty}{\to} 2c_0$$

for $c_0 = 2\sqrt{2}/3$.

PROOF: By a one-dimensional construction, we have the upper bound

$$L^{1-d} E[\text{minimal saddle}] \le c(L) \times 2 \underset{L\to\infty}{\to} 2c_0,$$

where $2c(L)$ is the energy of the minimal periodic saddle point in one dimension. For the lower bound, a min-max argument assures

$$E[\text{minimal saddle}] \ge \min_{\bar{u}=0} E[u].$$

(There must be a mean zero state along any path from one minimizer to the other.) Therefore,

$$L^{1-d} E[\text{minimal saddle}] \ge L^{1-d} \min_{\bar{u}=0} E[u] \underset{L\to\infty}{\to} c_0 P = 2c_0.$$

Here, P denotes the minimal perimeter of a surface bounding half the volume of a periodic cube in d dimensions. The convergence follows from the work of Modica and Mortola [26, 27]. The last step uses an isoperimetric inequality of Hadwiger [19], which reveals that the minimal perimeter of a system with volume

$\frac{1}{2}$ on the periodic lattice is $P = 2$. For more about isoperimetric inequalities, see also [34]. □

Remark B.6. The limit of the energy of the minimal saddle is achieved by one-dimensional constructions. We conjecture that for periodic boundary conditions, the minimal saddles at finite L are in fact one-dimensional.

Acknowledgments. We thank Weinan E, Weiqing Ren, and Yoshihiro Tonegawa for their comments and insight. This paper includes and extends some of the material from the doctoral dissertation [32]. R. V. Kohn was partially supported by National Science Foundation grants 0101439 and 0313744. F. Otto was partially supported by Deutsche Forschungsgemeinschaft through SFB 611. M. G. Reznikoff was supported by a National Science Foundation Mathematical Sciences Postdoctoral Research Fellowship. E. Vanden-Eijnden was partially supported by National Science Foundation grants DMS0101439, DMS0209959, and DMS0239625.

Bibliography

[1] Bellettini, G.; Mugnai, L. On the approximation of the elastica functional in radial symmetry. *Calc. Var. Partial Differential Equations* **24** (2005), no. 1, 1–20.

[2] Braides, A. *Γ-convergence for beginners.* Oxford Lecture Series in Mathematics and Its Applications, 22. Oxford University Press, Oxford, 2002.

[3] Braides, A.; March, R. Approximation by Γ-convergence of a curvature-depending functional in visual reconstruction. *Comm. Pure Appl. Math.* **59** (2006), no. 1, 71–121.

[4] Bronsard, L.; Kohn, R. V. On the slowness of phase boundary motion in one space dimension. *Comm. Pure Appl. Math.* **43** (1990), no. 8, 983–997.

[5] Carr, J.; Pego, R. L. Metastable patterns in solutions of $u_t = \epsilon^2 u_{xx} - f(u)$. *Comm. Pure Appl. Math.* **42** (1989), no. 5, 523–576.

[6] Chan, T. F.; Kang, S. H.; Shen, J. Euler's elastica and curvature-based inpainting. *SIAM J. Appl. Math.* **63** (2002), no. 2, 564–592.

[7] Da Prato, G.; Zabczyk, J. *Stochastic equations in infinite dimensions.* Encyclopedia of Mathematics and Its Applications, 44. Cambridge University Press, Cambridge, 1992.

[8] De Masi, A; Dirr, N.; Presutti, E. Instability of interface under forced displacements. Max-Planck-Institut für Mathematik. Preprint, 2005.

[9] de Mottoni, P.; Schatzman, M. Évolution géométrique d'interfaces. *C. R. Acad. Sci. Paris Sér. I Math.* **309** (1989), no. 7, 453–458.

[10] E, W.; Ren, W.; Vanden-Eijnden, E. Minimum action method for the study of rare events. *Comm. Pure Appl. Math.* **57** (2004), no. 5, 637–656.

[11] Esedoglu, S.; Shen, J. Digital inpainting based on the Mumford-Shah-Euler image model. *European J. Appl. Math.* **13** (2002), no. 4, 353–370.

[12] Evans, L. C.; Soner, H. M.; Souganidis, P. E. Phase transitions and generalized motion by mean curvature. *Comm. Pure Appl. Math.* **45** (1992), no. 9, 1097–1123.

[13] Faris, W. G.; Jona-Lasinio, G. Large fluctuations for a nonlinear heat equation with noise. *J. Phys. A* **15** (1982), no. 10, 3025–3055.

[14] Fogedby, H. C.; Hertz, J.; Svane, A. Domain wall propagation and nucleation in a metastable two-level system. *Phys. Rev. E* **70** (2004), 031105.

[15] Freidlin, M. I.; Wentzell, A. D. *Random perturbations of dynamical systems.* 2nd edition. Fundamental Principles of Mathematical Sciences, 260. Springer, New York, 1998.

[16] Funaki, T. The scaling limit for a stochastic PDE and the separation of phases. *Probab. Theory Related Fields* **102** (1995), no. 2, 221–288.

[17] Fusco, G.; Hale, J. K. Slow-motion manifolds, dormant instability, and singular perturbations. *J. Dynam. Differential Equations* **1** (1989), no. 1, 75–94.

[18] Gurtin, M. E.; Matano, H. On the structure of equilibrium phase transitions within the gradient theory of fluids. *Quart. Appl. Math.* **46** (1988), no. 2, 301–317.

[19] Hadwiger, H. Gitterperiodische Punktmengen und Isoperimetrie. *Monatsh. Math.* **76** (1972), 410–418.

[20] Hutchinson, J. E.; Tonegawa, Y. Convergence of phase interfaces in the van der Waals–Cahn–Hilliard theory. *Calc. Var. Partial Differential Equations* **10** (2000), no. 1, 49–84.

[21] Ilmanen, T. Convergence of the Allen-Cahn equation to Brakke's motion by mean curvature. *J. Differential Geom.* **38** (1993), no. 2, 417–461.

[22] Kohn, R. V.; Reznikoff, M. G.; Tonegawa, Y. The sharp-interface limit of the action functional for Allen Cahn in one space dimension. *Calc. Var. Partial Differential Equations*, in press.

[23] Kohn, R. V.; Reznikoff, M. G.; Vanden-Eijnden, E. Magnetic elements at finite temperature and large deviation theory. *J. Nonlinear Sci.* **15** (2005), 223–253.

[24] Kurzke, M. Boundary vortices in thin magnetic films. MPI MIS Preprint 14/2004. *Calc. Var. Partial Differential Equations*, in press.

[25] Luckhaus, S.; Modica, L. The Gibbs-Thompson relation within the gradient theory of phase transitions. *Arch. Rational Mech. Anal.* **107** (1989), no. 1, 71–83.

[26] Modica, L. The gradient theory of phase transitions and the minimal interface criterion. *Arch. Rational Mech. Anal.* **98** (1987), no. 2, 123–142.

[27] Modica, L.; Mortola, S. Il limite nella Γ-convergenza di una famiglia di funzionali ellittici. *Boll. Un. Mat. Ital. A (5)* **14** (1977), no. 3, 526–529.

[28] Moser, R. Ginzburg-Landau vortices for thin ferromagnetic films. *AMRX Appl. Math. Res. Express* **2003**, no. 1, 1–32.

[29] Moser, R. Boundary vortices for thin ferromagnetic films. *Arch. Ration. Mech. Anal.* **174** (2004), no. 2, 267–300.

[30] Moser, R. A higher order asymptotic problem related to phase transitions. *SIAM J. Math. Anal.* **37** (2005), no. 3, 712–736.

[31] Reshetnyak, Y. G. Weak convergence of completely additive vector functions on a set. *Siberian Math. J.* **9** (1968), 1039–1045; translated from Sibirskii Mathematicheskii Zhurnal **9** (1968), 1386–1394.

[32] Reznikoff, M. G. *Rare events in finite and infinite dimensions.* Doctoral dissertation, Courant Institute of Mathematical Sciences, 2004.

[33] Reznikoff, M. G.; Vanden-Eijnden, E. Rare events on large domains: a reduction of stochastic pde dynamics. In preparation.

[34] Ros, A. The isoperimetric problem. Lecture Notes at the Clay Mathematics Institute Summer School, Cambridge, Mass., 2001.

[35] Rubinstein, J.; Sternberg, P.; Keller, J. B. Fast reaction, slow diffusion, and curve shortening. *SIAM J. Appl. Math.* **49** (1989), no. 1, 116–133.

[36] Sandier, E.; Serfaty, S. Gamma-convergence of gradient flows with applications to Ginzburg-Landau. *Comm. Pure Appl. Math.* **57** (2004), no. 12, 1627–1672.

[37] Tonegawa, Y. Phase field model with a variable chemical potential. *Proc. Roy. Soc. Edinburgh* **132A** (2002), 993–1019.

[38] Varadhan, S. R. S. *Large deviations and applications.* CBMS-NSF Regional Conference Series in Applied Mathematics, 46. Society for Industrial and Applied Mathematics (SIAM), Philadelphia, 1984.

ROBERT V. KOHN
Courant Institute
251 Mercer Street
New York, NY 10012
E-mail: kohn@cims.nyu.edu

FELIX OTTO
Institut für Angewandte Mathematik
University of Bonn
Wegelerstraße 10
D-53115 Bonn
GERMANY
E-mail: otto@iam.uni-bonn.de

MARIA G. REZNIKOFF
Institut für Angewandte Mathematik
University of Bonn
Wegelerstraße 10
D-53115 Bonn
GERMANY
E-mail: reznikoff@iam.uni-bonn.de

ERIC VANDEN-EIJNDEN
Courant Institute
251 Mercer Street
New York, NY 10012
E-mail: eve2@cims.nyu.edu

Received March 2005.